Atmosphere **2014**, *5*, 342-369; doi:10.3390/atmos5020342

OPEN ACCESS

atmosphere

ISSN 2073-4433

www.mdpi.com/journal/atmosphere

Article

Mercury Plumes in the Global Upper Troposphere Observed during Flights with the CARIBIC Observatory from May 2005 until June 2013

Franz Slemr [1,*], Andreas Weigelt [2], Ralf Ebinghaus [2], Carl Brenninkmeijer [1], Angela Baker [1], Tanja Schuck [1,†], Armin Rauthe-Schöch [1], Hella Riede [1], Emma Leedham [1], Markus Hermann [3], Peter van Velthoven [4], David Oram [5], Debbie O'Sullivan [5,‡], Christoph Dyroff [6], Andreas Zahn [6] and Helmut Ziereis [7]

[1] Atmospheric Chemistry Division, Max-Planck-Institut für Chemie (MPI), Hahn-Meitner-Weg 1, D-55128 Mainz, Germany; E-Mails: carl.brenninkmeijer@mpic.de (C.B.); angela.baker@mpic.de (A.B.); tanja.schuck@mpic.de (T.S.); armin.rauthe-schoech@mpic.de (A.R.-S.); hella.riede@mpic.de (H.R.); emma.leedham@mpic.de (E.L.)

[2] Institute of Coastal Research, Helmholtz-Zentrum Geesthacht (HZG), Max-Planck-Straße 1, D-21502 Geesthacht, Germany; E-Mails: andreas.weigelt@hzg.de (A.W.); ralf.ebinghaus@hzg.de (R.E.)

[3] Leibniz-Institut für Troposphärenforschung (TROPOS), Permoserstrasse 15, D-04318 Leipzig, Germany; E-Mail: hermann@tropos.de.

[4] Royal Netherlands Meteorological Institute (KNMI), P.O. Box 201, NL-3730 AE De Bilt, The Netherlands; E-Mail: velthove@knmi.nl.

[5] National Centre for Atmospheric Science, University of East Anglia (UEA), Norwich NR4 7TJ, UK; E-Mails: d.oram@uea.ac.uk (D.O.); debbie.osullivan@metoffice.gov.uk (D.O.S.)

[6] Institute of Meteorology and Climate Research, Karlsruhe Institute of Technology (KIT), Hermann-von-Helmholtz-Platz 1, D-76344 Eggenstein-Leopoldshafen, Germany; E-Mails: christoph.dyroff@kit.edu(C.D.); andreas.zahn@kit.edu (A.Z.)

[7] Institut für Physik der Atmosphäre, Deutsches Zentrum für Luft- und Raumfahrt (DLR), D-82230 Wessling, Germany; E-Mail: helmut.ziereis@dlr.de

† Current Affiliation: NRW State Agency for Nature, Environment and Consumer Protection, Recklinghausen, Germany

‡ Current Affiliation: Meteorological Office, Exeter, EX1 3PB, UK

* Author to whom correspondence should be addressed; E-Mail: franz.slemr@mpic.de; Tel.: +49-8821-52595.

Received: 24 February 2014; in revised form: 28 April 2014 / Accepted: 30 April 2014 / Published: 28 May 2014

Abstract: Tropospheric sections of flights with the CARIBIC (Civil Aircraft for Regular Investigation of the Atmosphere Based on an Instrumented Container) observatory from May 2005 until June 2013, are investigated for the occurrence of plumes with elevated Hg concentrations. Additional information on CO, CO_2, CH_4, NOy, O_3, hydrocarbons, halocarbons, acetone and acetonitrile enable us to attribute the plumes to biomass burning, urban/industrial sources or a mixture of both. Altogether, 98 pollution plumes with elevated Hg concentrations and CO mixing ratios were encountered, and the Hg/CO emission ratios for 49 of them could be calculated. Most of the plumes were found over East Asia, in the African equatorial region, over South America and over Pakistan and India. The plumes encountered over equatorial Africa and over South America originate predominantly from biomass burning, as evidenced by the low Hg/CO emission ratios and elevated mixing ratios of acetonitrile, CH_3Cl and particle concentrations. The backward trajectories point to the regions around the Rift Valley and the Amazon Basin, with its outskirts, as the source areas. The plumes encountered over East Asia and over Pakistan and India are predominantly of urban/industrial origin, sometimes mixed with products of biomass/biofuel burning. Backward trajectories point mostly to source areas in China and northern India. The Hg/CO_2 and Hg/CH_4 emission ratios for several plumes are also presented and discussed.

Keywords: mercury; emission; air; pollution

1. Introduction

Mercury (Hg) is emitted by natural and anthropogenic processes, and because of its rather long atmospheric lifetime of one year, it can be transported over long distances [1,2]. After oxidation and deposition, part of it can be transformed to highly neurotoxic methyl mercury. The latter is then bio-accumulated in the aquatic food web and may harm both human populations and fauna, which are dependent on fish [3,4]. Emissions from different natural and anthropogenic processes, such as volcanic emissions, emission from the oceans, from soils, coal and biomass burning, as well as many other anthropogenic activities, have been estimated, and spatially and temporally resolved emission inventories have been calculated from the emission factors obtained in these studies (e.g., [5–15]). Despite all these efforts, the emission estimates are still quite uncertain, especially those related to natural sources and anthropogenic emissions in rapidly developing countries in East and South-East Asia [9,13,16,17]. Thus, more data on mercury emissions are required, and the existing inventories need to be evaluated by measurements.

Direct measurements of emissions by techniques, such as a mass balance technique or using an artificially emitted tracer substance [18], are complex and expensive. The mass balance technique

measures the fluxes in and out of a chosen source area and calculates the emissions as a difference between them. For a middle-sized city, it requires the use of several aircraft equipped with precise chemical and meteorological instrumentation to resolve small differences of large fluxes. Alternatively, an artificial tracer, such as SF_6, is emitted in an area under investigation and the emission of the target substance is calculated from the known emission of the artificial tracer and the correlations of the target substance concentrations with those of the tracer. Both techniques have been successfully used to determine emissions of CO and NOy of a middle-sized city [18], but they can hardly be scaled up to larger areas. A determination of emission ratios of two substances from their concentrations in the plumes even of large areas is experimentally much more amenable [18–20]. Consequently, emission ratios are promising to be the most practicable way to evaluate the consistency of an emission inventory of one substance with an inventory of another substance [21]. Emission ratios can also be used to constrain the lesser known emissions of one substance using the better known emissions of another substance [21,22].

The CARIBIC (Civil Aircraft for Regular Investigation of the Atmosphere Based on an Instrumented Container) observatory is a long-term project aimed at the monitoring of atmospheric composition and its changes by using an instrumented freight container flown on-board a passenger aircraft during intercontinental flights [23]. It started in 1997 and, apart from an interruption between 2002 and 2004, has been operational continuously over more than 15 years. Despite cruising most of the time at altitudes from 10 to 12 km, plumes of polluted air lifted mostly by convection or warm conveyor belts [24,25] are frequently encountered in the tropospheric sections of the flights.

Here, we report on plumes with elevated mercury concentrations observed during CARIBIC flights since May 2005, when a mercury instrument was installed until June 2013. Rich ancillary data on other gases, such as carbon monoxide (CO), carbon dioxide (CO_2), methane (CH_4), total reactive nitrogen (NOy), hydrocarbons, halocarbons and on atmospheric aerosol, enable a detailed characterization of the plumes, its attribution to the emission processes and, in combination with backward trajectories, an approximate localization of the emissions. Correlations of Hg with CO, CO_2 and CH_4 provide Hg/CO, Hg/CO_2 and Hg/CH_4 emission ratios, which may help to constrain the estimates of mercury emissions using the CO, CO_2 and CH_4 emission inventories [21].

2. Experimental Section

Since December 2004, a new CARIBIC measurement container [23] on-board an Airbus 340–600 of Lufthansa has been flown monthly on transcontinental flights. The corresponding routes (until June 2013) are shown in Figure 1, and the complete list of flights can be found at www.caribic-atmospheric.com. Typically, a sequence of 4 consecutive intercontinental flights is executed every month. The modified freight container (gross weight: 1.5 metric tons) holds 15 automated analysers for the *in situ* measurements of mercury concentrations and mixing ratios of CO, O_3, NO, NOy, CO_2, total (including cloud droplets) and gaseous water, oxygenated organic compounds and concentrations of fine particles (three counters for particles with diameters >4 nm, >12 nm and >18 nm, all up to 2 μm), as well as one optical particle counter for particles with diameters of 130–900 nm. In addition, air and aerosol samples are taken in flight and subsequently analysed in the laboratory for greenhouse gases, halocarbons, non-methane hydrocarbons (NMHCs) and particle elemental composition and

morphology, respectively [23]. In May 2010, several instruments were upgraded and new instruments were added. In the context of this paper, the most important change was the addition of a whole air sampler with a capacity of 88 samples and of an instrument for continuous measurements of CH_4 (Fast Greenhouse Gas Analyzer, Los Gatos Research, [26]). With the new whole air sampler, the measurement frequency of greenhouse gases [27] and hydrocarbons [28] could be increased from 28 to 116 measurements per flight sequence. Halocarbon measurements (except for CH_3Cl, which can be determined by both hydrocarbon and halocarbon analytical methods) were unaffected, due to the limited volume of air available for analysis in the new sampler.

Figure 1. The tracks of 328 CARIBIC (Civil Aircraft for Regular Investigation of the Atmosphere Based on an Instrumented Container) flights from May 2005 until June 2013. The colours denote the classification of destination airports used in this paper: green, East Asia; yellow, South Asia; light blue, Africa; dark blue, South America; red, North America.

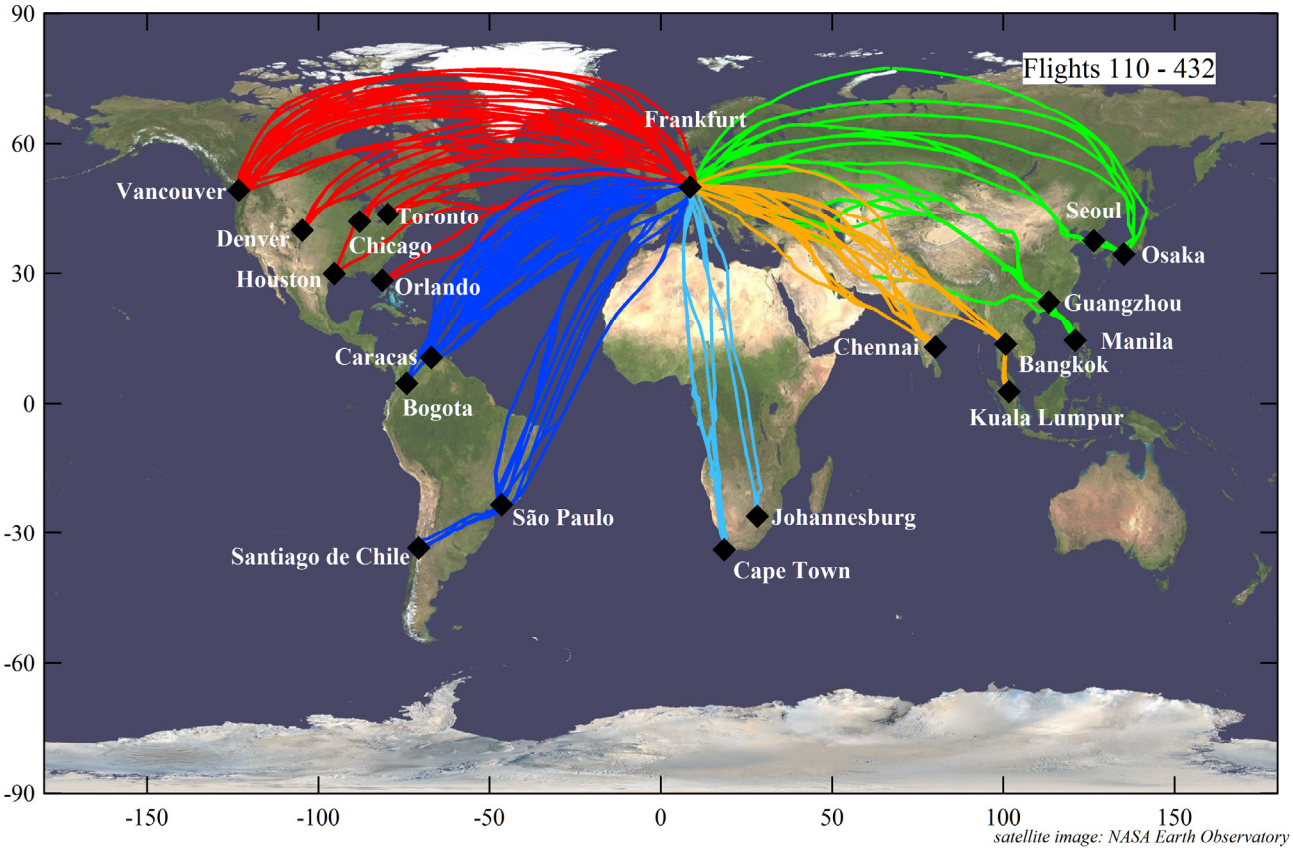

The air and aerosol inlet system and instrument tubing are described in detail by Brenninkmeijer *et al.* [23] and Slemr *et al.* [29]. Briefly, the trace gas probe consists of a 3-cm inner diameter diffuser tube with a forward facing inlet orifice of 14 mm in diameter and an outlet orifice of 12 mm in diameter, providing an effective ram pressure of about 90–170 hPa, depending on cruising altitude and speed. This ram pressure forces about 100 L/min of ambient air through a PFA tubing heated to 40 °C (a 3 m-long, 16-mm ID PFA-lined tube connecting the inlet and the container and 1.5 m-long, 16-mm ID PFA tubing within the container to the instrument manifold). The sample air for the mercury analyser is taken at a flow rate of 0.5 L(STP, *i.e.*, at standard temperature of 273.15 K and

pressure of 1013.25 hPa)/min from the manifold using 4-mm ID PFA tubing heated by the energy dissipated in the container to ~30 °C. The arrangement similar to that described by Talbot *et al.* [30] was optimized to transmit highly surface reactive HNO_3 [31] and can thus be presumed to facilitate the transfer of gaseous oxidized mercury (GOM), as well [30]. The large flow through the trace gas diffuser inlet tube of more than 2000 L/min and perpendicular sampling at much smaller flow rates of about 100 L/min discriminate against particles larger than about one micrometre in diameter (50% aspiration efficiency [32]). Consequently, all smaller particles and, thus, the major fraction of particle mass in the upper troposphere will be transported to the manifold in the container.

The mercury instrument, which is based on an automated dual channel, single-amalgamation, cold vapour atomic fluorescence analyser (Tekran-Analyzer Model 2537 A, Tekran Inc., Toronto, ON, Canada), is described by Slemr *et al.* [29]. The instrument features two gold cartridges. While one is adsorbing mercury during a sampling period, the other is being thermally desorbed using argon as a carrier gas. Hg is detected using cold vapour atomic fluorescence spectroscopy (CVAFS). The functions of the cartridges are then interchanged, allowing continuous sampling of the incoming air stream. A 45-mm diameter PTFE pre-filter (pore size 0.2 μm) protects the sampling cartridges against contamination by particles that pass through the inlet system. The 0.5 L(STP)/min of air sample, typically at 200–300 hPa, is compressed to about 500 hPa, needed to operate the instrument with its internal pump. Extensive laboratory tests of this PTFE diaphragm pump (KNF-Neuberger, Model N89KTDC) did not show either any contamination of the system with Hg or Hg losses. To avoid the contamination of the instruments and of the tubing connecting the sampling manifold with the instruments during ascents and descents in polluted areas near airports, the sampling pumps are activated only at an ambient pressure below 500 hPa. Consequently, no measurements below an altitude of about 5 km were made.

Initially, the instrument was operated with a gas mixture of 0.25% CO_2 in argon, which also is used for the operation of the CO instrument. Because the addition of CO_2 to argon reduced the sensitivity of the fluorescence detector by ~35%, the instrument was run initially with a 15-min sampling time (corresponding to a ~225 km-flying distance) until March 2006 (Flight 145) and with 10 min until June 2007 (Flight 197). Since August 2007, the CO_2 has been removed from the gas mixture using a tube filled with an X10 molecular sieve. The corresponding sensitivity gain enabled us to reduce the sampling interval to 5 min (corresponding to a ~75-km flying distance). The instrument is calibrated after every other month in the laboratory by ~48 h of parallel operation to a well-calibrated identical instrument. A detection limit of ~0.1 ng·Hg·m^{-3} and a reproducibility of about 0.05 ng·Hg·m^{-3} is achieved at our operating conditions. To improve the detection limit and reproducibility of the measurements, we returned to 10-min sampling in August 2011 (Flight 349). For this paper, the data from May 2005 to June 2013, were analysed. All mercury concentrations are reported in ng·Hg·m^{-3} (STP, *i.e.*, at 1013.25 hPa and 273.15 K).

Speciation experiments on-board the CARIBIC container, where gaseous oxidized mercury (GOM) was removed in the instrument using a KCl or soda lime trap upstream of one of the gold cartridges, showed qualitatively that GOM (essentially Hg^{2+}) is transmitted through the inlet system to the instrument and will be measured. A demonstration of a quantitative transmission would require capabilities to prepare GOM test mixtures at high flow rates and to replicate the flight conditions (*i.e.*, −50 °C, 900 km·h^{-1}), which is beyond the constraints imposed by a commercial airliner.

Temme *et al.* [33] found the GOM transmission to be quantitative at conditions similar to those in the upper troposphere, *i.e.*, low temperatures and dry air, which allows us to assume the same for our system. A definitive verification of this assumption has to wait for an in-flight intercomparison with a research aircraft with proven speciation capabilities. Newer data on the gas-particle partitioning of atmospheric Hg^{2+} [34,35] suggest that particle bound mercury (PBM, also mostly Hg^{2+}) sampled near the tropopause at temperatures of ~−50 °C will evaporate when warmed up to ~+40 °C during the transport in the sampling tubing to the instrument. PBM on particles that make it into the trace gas inlet will thus be most likely also measured. Consequently, the CARIBIC measurements approximate the total mercury concentration in the troposphere. We note that even if GOM concentrations in the upper troposphere represent more than 1% or less of total gaseous mercury concentrations typically found in the boundary layer [36,37], its non-quantitative transmission by our inlet system would not substantially influence the results presented in this paper.

The plumes with elevated Hg concentrations showed, apart from a few exceptions mentioned in Section 3.1, also elevated CO and, sometimes, CO_2 and CH_4 mixing ratios. For these plumes, the Hg/CO, Hg/CO_2 and Hg/CH_4 emission ratios were calculated by bivariate least-squares correlations of Hg with CO, CO_2 and CH_4 [38], respectively, which take into account the uncertainties in both variables. For these correlations, the continuously measured CO, CO_2 and CH_4 were averaged over the Hg sampling interval. The uncertainties of Hg, CO, CO_2 and CH_4 measurements were set to 0.05 pg·m^{-3}, 1 ppb, 0.05 ppm and 3 ppb, respectively. The underlying assumptions in the emission ratio calculations are: (1) that none of the correlated substances are lost during the transport from the source to the point of encounter by chemical reactions; (2) that the emission ratios are nearly constant during the observation interval; and (3) that the plume is embedded in a homogeneous air mass, *i.e.*, that the Hg concentration and CO, CO_2 or CH_4 mixing ratios before and after the plume are nearly the same [20]. Assumption (1) is fulfilled, as the transport times (ranging from a few days to about one week) are much shorter than the atmospheric lifetime of our target compounds (CO has the shortest lifetime of ~2 months, with a local lifetime in the tropics being several weeks). Assumptions (2) and (3) are probably fulfilled for a majority of smaller plumes. The large plumes stretching over thousands of kilometres north and south of the intertropical convergence zone (ITCZ) during the flights to South Africa are superimposed on a north-south Hg gradient, which violates Assumption (3). Sometimes, large overlapping plumes with different sources in different areas are sampled, also violating the Assumption (2). Consequently, even statistically significant Hg *vs.* CO, CO_2 and CH_4 correlations may sometimes provide biased Hg/CO, Hg/CO_2 or Hg/CH_4 emission ratios in the case of the African flights.

Meteorological analyses for all CARIBIC flights are provided by KNMI (Royal Netherlands Meteorological Institute) at http://www.knmi.nl/samenw/CARIBIC. Trajectories were calculated at 3-min intervals along the flight track for each flight with the KNMI trajectory model, TRAJKS [39], using data from ECMWF (European Centre for Middle Weather Forecast) data.

3. Results and Discussion

3.1. Overview

Compared to the search for plumes at a ground station [21], the processing of the CARIBIC data is complicated by the variability of the data over large distances in the upper troposphere and by the

frequent changes of tropospheric and stratospheric air masses. Figure 2 shows an overview of the data from Flight 158 from Frankfurt to Guangzhou on 31 July and 1 August 2006. The aircraft flew in the troposphere until ~23:00 UTC and then in the stratosphere until about 1:45 UTC on 1 August. The stratospheric section is evidenced by the high potential vorticity and O_3 mixing ratio, as well as the low CO mixing ratio shown in the upper two panels of the data time series. In the tropospheric section after about 1:45 UTC on 1 August 2006, mercury background concentrations vary between about 1.25 and 1.35 $ng \cdot m^{-3}$ (the second panel from the top of the data time series). Three events with elevated Hg concentrations, denoted as A, B and C, with peak Hg concentrations of 1.55, 1.5 and 2.3 $ng \cdot m^{-3}$ are observed at about 2:40, 4:50 and 6:00 UTC, respectively, on 1 August 2006. All events are accompanied by elevated CO (the second panel from the top), NOy, H_2O (middle panel) and acetone (bottom panel). We base our approach on the visual inspection of the data overview plots of each flight for the coincident occurrence of elevated Hg concentrations with elevated CO mixing ratios. Plumes identified in this way are cross-checked using variations of other tracers for anthropogenic emissions, such as NOy (middle panel), acetone (bottom panel), CH_4 (the second panel from the bottom), non-methane hydrocarbons (not available for this flight) and halocarbons (the second panel from the bottom). Humidity and cloud water content (determined as the difference between total water content and the water vapour mixing ratio) as tracers for convective processes are also sometimes useful.

An event within the stratospheric section of the flight at ~23:25 UTC (marked as D) has a similar characteristics as Events A, B and C and can easily be mistaken for a plume. The only pronounced difference is that the maximum of Hg concentration (and CO, acetone and H_2O mixing ratios) in Event D coincides with dips in potential vorticity and O_3 mixing ratios, both at higher levels characteristic for the lower stratosphere. Such dips in potential vorticity and O_3 indicate a crossing of a filament of tropospheric air in the stratosphere. The variation of all mentioned species during such crossing results from their strong gradients above the tropopause [29]. Events of this type are thus not related to surface emissions and have to be eliminated from further consideration. Consequently, only events embedded in air with a potential vorticity of less than 1.5 PVU (1 PVU = $10^{-6} \cdot m^2 \cdot K \cdot kg^{-1} \cdot s^{-1}$) and/or less than 150 ppb O_3 were considered.

Because we rely mostly on Hg and CO as plume tracers, only those processes that emit Hg and CO, such as biomass burning, will be detected. This includes also collocated emissions of Hg and CO, CO_2 or CH_4, which applies for most of the urban and industrial emissions. However, emissions from mining and smelting, which emit hardly any CO, CO_2 or CH_4, will not be detected (unless collocated with other CO, CO_2 or CH_4 sources), because a suitable specific tracer for these processes, such as SO_2, is not on the otherwise comprehensive list of CARIBIC *in situ* measurements. Lacking *in situ* SO_2 measurements also prevents the direct detection and identification of volcanic Hg emissions. One such SO_2 plume was detected during the descent to Frankfurt airport on 15 August 2008, using remote SO_2 sensing by a nadir looking differential optical absorption system (DOAS) on-board CARIBIC and remote sensing satellite [40]. Quantitative evaluation of this plume in terms of Hg emission, however, was not possible, because the DOAS measurement does not provide *in situ* SO_2 concentrations and the elevated Hg concentrations were documented by only one Hg measurement point. Among the substances measured in the whole air samples are tracers for marine emissions, such as short-lived bromine and iodine containing halocarbons, but the low sampling frequency (28 samples taken over

four intercontinental flights) makes them unsuitable as tracers for the detection of the Hg plumes of marine origin. ^{222}Rn as a tracer for terrestrial Hg emissions [22] is also not being measured on-board CARIBIC. Consequently, in this study, we can only distinguish between Hg plumes of biomass burning or urban/industry origin.

The short encounter with the Kasatochi volcano plume (~5 min) in 2008 during the descent to Frankfurt airport [40] also illustrates some practical limits of our approach. The most severe limitation is given by the low temporal resolution of the Hg measurements of 5–15 min corresponding to a ~75–225 km flight distance. Statistically significant Hg *vs.* CO, CO_2 and CH_4 correlations require at least three measurements. Thus, only plumes larger than ~300 km can be captured by our approach, which also means that many plumes encountered during the short aircraft ascents and descents cannot be resolved. The CARIBIC measurements start and stop at ~500 hPa to prevent the contamination of the CARIBIC system by polluted air in the boundary layer near the airports [23]. Consequently, information for the boundary layer, the most polluted part of the troposphere, is missing in our data set. In addition, the Hg, CO, CO_2 and CH_4 data from ascents and descents through quasi-horizontal layers in the troposphere are likely to violate the assumption of a plume being embedded in a homogeneous air mass on which the Hg *vs.* CO, CO_2 and CH_4 correlations are based.

Although almost all of the Hg plumes were accompanied by elevated CO mixing ratios, seven of them were observed during flight sections with nearly constant CO mixing ratios. All of these plumes were encountered over the equatorial Atlantic Ocean between 0° and 15° N during the flights to South American destinations. They were embedded in background mercury concentrations varying between ~0.95 and 1.3 ng·m^{-3}, and the elevation above the background (ΔHg) varied between ~0.25 and 0.45 ng·m^{-3}. In these events, elevated Hg concentrations were always accompanied by elevated humidity, frequently also with clouds and elevated NOy, as well as with low O_3 mixing ratios; frequently, only around 30 ppb. Such low O_3 mixing ratios are typical for the marine boundary layer over the equatorial Atlantic Ocean [41]. Backward trajectories reveal contact with the equatorial Atlantic Ocean surface. Satellite images of cloud cover indicate that these events are due to the convection of the air masses from the marine boundary layer at the ITCZ. Elevated Hg concentration in these events encountered in the upper free troposphere can point to emissions of mercury by ocean [42], but we lack highly resolved tracer data for air from the marine boundary layer to quantitatively describe them.

Despite these caveats and limitations, 98 encounters with plumes with elevated CO mixing ratios and simultaneously elevated Hg concentrations were counted during 309 CARIBIC flights with valid Hg measurements between May 2005 and June 2013. Taking into account the number of flights to the respective regions listed in Table 1, the probability of plume encounters was highest during the flights to South Africa with 85% of the flights. The second highest probability of plume occurrence was over East Asia with 46%, followed by flights to South Asia with 26%, South America with 20% and North America with 17%. The low frequency of plume encounters over North America is partly due to the high northern latitude of the flight routes of these flights, which, at usual flight altitudes of 10–12 km, results in a high proportion of stratospheric sections with a potential vorticity >1.5 PVU. However, the high frequency of plume encounters during the flights to Osaka and Seoul with flight routes at similarly high northern latitudes shows that this bias alone cannot explain the low frequency of plume encounters over Europe and North America.

Figure 2. Overview of the data from Flight 158 from Frankfurt to Guangzhou on 31 July 2006. (**Top**) Flight track and the locations of whole air samples. Time series plots are below: (**uppermost panel**): flight altitude (magenta) and latitude (black), potential vorticity (blue), sampling intervals (grey bars); (**second panel from top**): mixing ratios of CO (black), O_3 (green) and Hg concentrations (red); (**middle panel**): mixing ratios of NO (black), NOy (red) and total water content (blue); (**second panel from bottom**): mixing ratios of CH_4 (blue), CH_3Cl (olive green) and CFC12 (CCl_2F_2, magenta)) in whole air samples; (**bottom panel**): mixing ratios of acetone (green) and CO_2 (blue). The three identified plumes are marked with A, B and C in the second panel from top. Another event, due to a crossing of a filament of tropospheric air within the lower stratosphere, is marked with D. Although similar to Events A, B and C, this event has no relation to surface emissions (see the text).

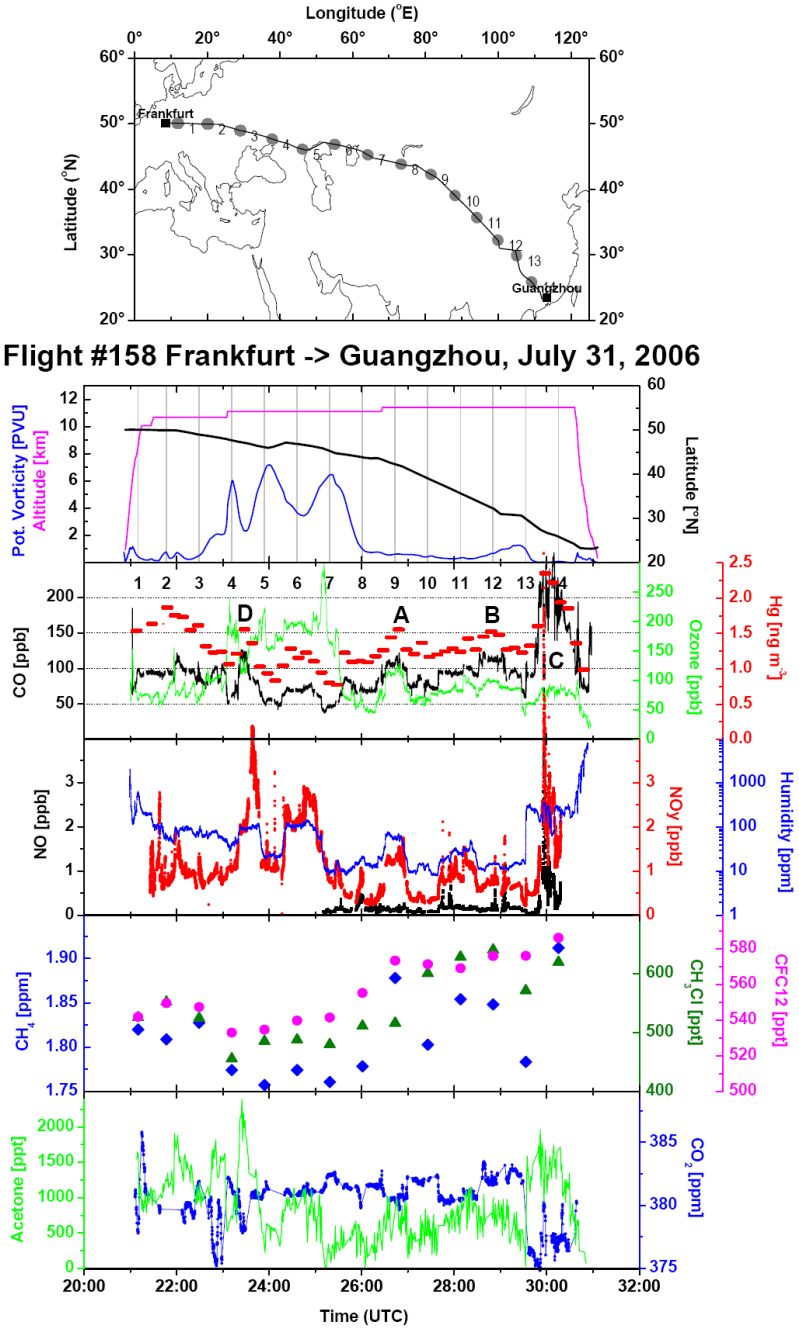

For 56 plume encounters (out of 98), the Hg *vs.* CO correlations were statistically significant at a confidence level of at least 95%. For these correlations, data from the same plume encountered twice in the vicinity of an airport were combined, e.g., for a plume near Guangzhou encountered during the forward and return flight to Manila (Flights 203 and 204) or a plume encountered near São Paulo during Flights 123 (Frankfurt→São Paulo), 124 (São Paulo→Santiago de Chile) and 125 (Santiago de Chile→São Paulo). Seven extremely high Hg/CO slopes of 12.9–23.7 $pg \cdot m^{-3} \cdot ppb^{-1}$ were connected with physically unrealistic negative intercepts and are thus eliminated from the data set, leaving 49 plume encounters with valid Hg/CO slopes. The geographic distribution of these plumes is shown in Figure 3.

Table 1. Overview of encounters with plumes with elevated Hg concentrations and CO mixing ratios.

Destination Airport	Number of Flights	Number of Plume Encounters	Number of Plumes With Significant Hg *vs.* CO Correlations	Median and Range of Hg/CO Emission Ratios ($pg \cdot m^{-3} \cdot ppb^{-1}$)
South Africa	13	11	4	2.9 (2.2–7.5)
East Asia	101	46	31	8.2 (2.3–16.6)
South Asia	57	15	6	7.4 (5.0–10.0)
South America	90	18	5	1.3 (1.1–3.3)
North America	48	8	2	9.2 (6.9 and 11.4)

Figure 3. Geographic distribution and the extension of the plumes with statistically significant Hg *vs.* CO correlations. The magnitude of Hg/CO emission ratios in $pg \cdot m^{-3} \cdot ppb^{-1}$ is colour coded.

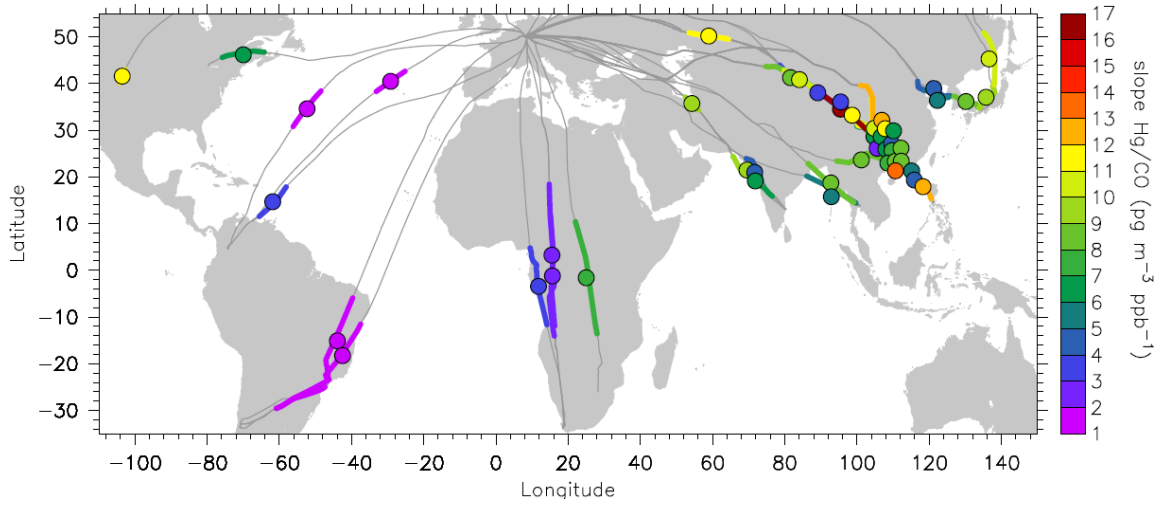

Most of the plumes with statistically significant Hg *vs.* CO correlations (31 plumes) were encountered over the East Asian region, and these are listed in Table S1 (Supplementary Information). Table S2 lists 18 plumes with statistically significant Hg *vs.* CO correlations for all other regions. Relative to the number of flights, the frequency of plumes with statistically significant Hg/CO correlations is the highest for the South African and East Asian flights, with each being 31%, followed by flights to South Asia with 11%, South America with 6% and North America with 4%. The high

occurrence of plumes during the flights to South Africa in which Hg does not correlate with CO is caused by their large extension over a few thousands of km, changing the Hg and CO background from north to south hemispheric concentrations and the inhomogeneity of the plumes. This will be discussed later in Section 3.3.

The colour code of Figure 3 reveals a pronounced difference between the Hg/CO emission ratios in different regions. The Hg/CO emission ratios for plumes encountered over East Asia range from 2.3 to 16.6 pg·m^{-3}·ppb^{-1} (median 8.2 pg·m^{-3}·ppb^{-1}) and are similar to those over South Asia, ranging from 5.0 to 10.0 pg·m^{-3}·ppb^{-1} (median 7.4 pg·m^{-3}·ppb^{-1}). On the contrary, the Hg/CO emission ratios for plumes observed during the flights to South America and equatorial Africa range from 1.1 to 7.4 pg·m^{-3}·ppb^{-1}, with a median value of 1.8 pg·m^{-3}·ppb^{-1} (a median of 1.3 pg·m^{-3}·ppb^{-1} for South America and 2.9 pg·m^{-3}·ppb^{-1} for equatorial Africa). These plumes include also two plumes encountered over the Atlantic Ocean, which, based on backward trajectories, can be attributed to forest fires in the USA, as will be discussed in Section 3.4. The range and median of Hg/CO emission ratios observed over South America and equatorial Africa is similar to the one for plumes observed at Cape Point in South Africa [21]. A compilation of previously published Hg/CO emission ratios reported for different processes and regions [29] shows that biomass burning is characterized by ratios below 2 pg·m^{-3}·ppb^{-1} [43], whereas the ratios for urban/industrial emissions tend to be around 6 pg·m^{-3}·ppb^{-1} and higher. Applying these criteria to the Hg/CO emission ratios shown in Figure 3 thus leads to the conclusion that the plumes encountered during the flights to South America and equatorial Africa originate predominantly from biomass burning (see also [44]), whereas the plumes observed over East Asia, South Asia and North America are of industrial/urban or mixed origin. This preliminary classification is supported by the detailed discussion in Sections 3.2–3.4.

CO_2 emissions are better known than those of CO, and thus, the Hg/CO_2 emission ratios have a potential to provide a more accurate estimate of Hg emissions [21]. Unfortunately, CO_2 data were available for only 69 (out of 98) of the encountered plumes, of which nine were too narrow for Hg *vs.* CO_2 correlations. Statistically significant correlations of Hg *vs.* CO_2 were only found for the 17 plumes listed in Table S3. These correlations will be discussed in Section 3.5.

Mercury was also found to correlate frequently with methane at Cape Point, which proved to be useful for constraining the mercury emissions in South Africa [21]. Methane data were available only for flights since October 2010, and altogether, 26 correlations of Hg *vs.* CH_4 could be calculated, of which, only the six listed in Table S4 were statistically significant. These will be discussed in Section 3.6.

3.2. Plumes Encountered during the East Asian Flights

The East Asian plumes were encountered during the flights from Frankfurt to Manila with a stopover at Guangzhou and during the flights to Osaka and Seoul. Apart from a few plumes over Central Asia, most of them were encountered within a ~2000-km distance from the airports at Guangzhou, Osaka and Seoul. Data from one of the flights have already been shown in Figure 2. The Hg/CO emission ratios were 8.8 ± 1.5, 11.3 ± 2.0 and 7.49 ± 1.0 pg·m^{-3}·ppb^{-1} for Events A, B and C, respectively. Air sample analyses (the second panel from the bottom) show high CH_4 in Sample 9 (Event A, sample numbers are marked in the uppermost panel), 11 and 12 (Event B),

and the highest level in Sample 14 (Event C). Acetonitrile as a tracer for biomass burning is not available for this flight section, but elevated CH_3Cl mixing ratios (dark green triangles in the second panel from the bottom) indicate some influence of biomass/biofuel burning in Samples 10, 11, 12 and 14, but not in Sample 9. Backward trajectories for the preceding eight days for Samples 9, 11 and 12 in Figure 4 all show that transport took place at a higher altitude (<250 hPa). Notwithstanding, elevated H_2O mixing ratios and satellite cloud images (not shown) indicate convection in the area above the Persian Gulf and the Gulf of Oman for Samples 9 and 11 and above the Iberian Peninsula for Sample 12. Backward trajectories for Sample 14 had a surface contact over Sichuan, China. Fire maps (not shown) show fire counts in Oman and the Indus River Valley, which are reached by the trajectories of Sample 11, but not of 9. The biomass burning contribution for Sample 12 probably originates from fire activity in north-western Spain. No fire counts were reported for Sichuan during this period, but the observed influence of biomass burning could originate from biofuel use.

The composition and origin of the plumes over southern China and the Philippines (around the airport of Guangzhou, east of 103° E and south of 32° N) were analysed in detail by Lai *et al.* [45]. According to their chemical signatures, the 51 identified high CO events were attributed to biomass/biofuel burning, anthropogenic emissions or a mixture of both. The backward trajectories pointed to three source areas, namely: southern China, the Indochinese Peninsula and the Philippines/Indonesia. The emissions from southern China were found to be dominated by urban/industrial emissions, while emissions from biomass/biofuel burning contributed substantially to plumes from the Indochinese Peninsula. Mixed emissions were attributed to plumes originating from the Philippines/Indonesia.

Figure 4. Eight-day backward trajectories for whole air Samples 9 (**a**), 11 (**b**), 12 (**c**) and 14 (**d**) taken during Flight 158.

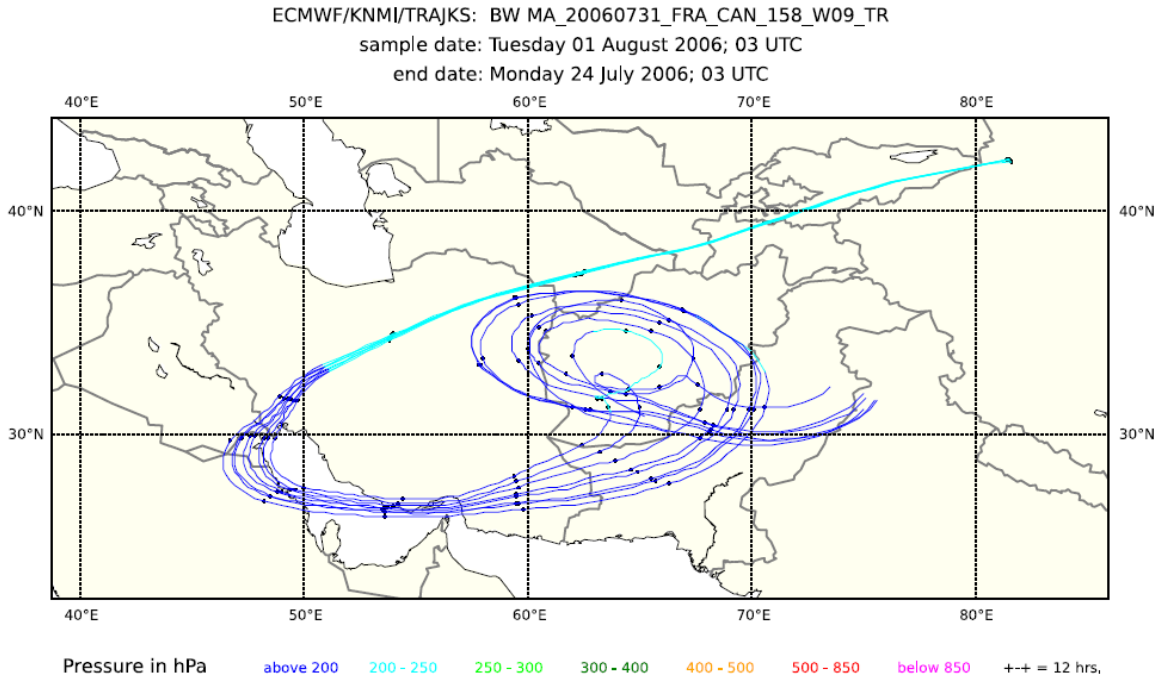

(**a**)

Figure 4. *Cont.*

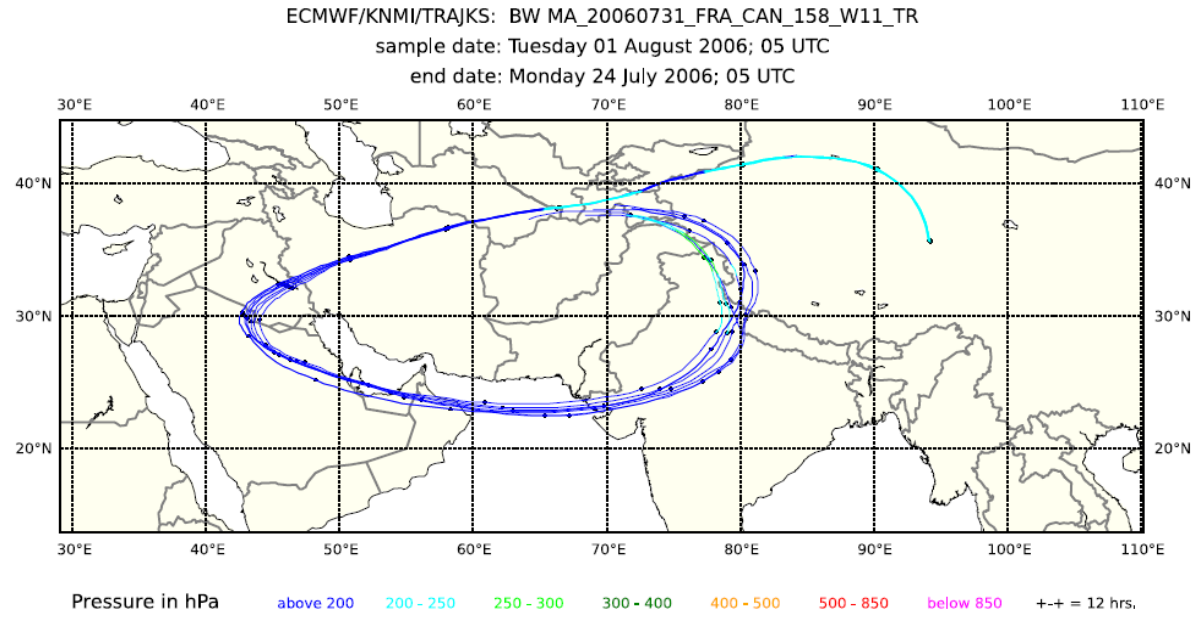

(b)

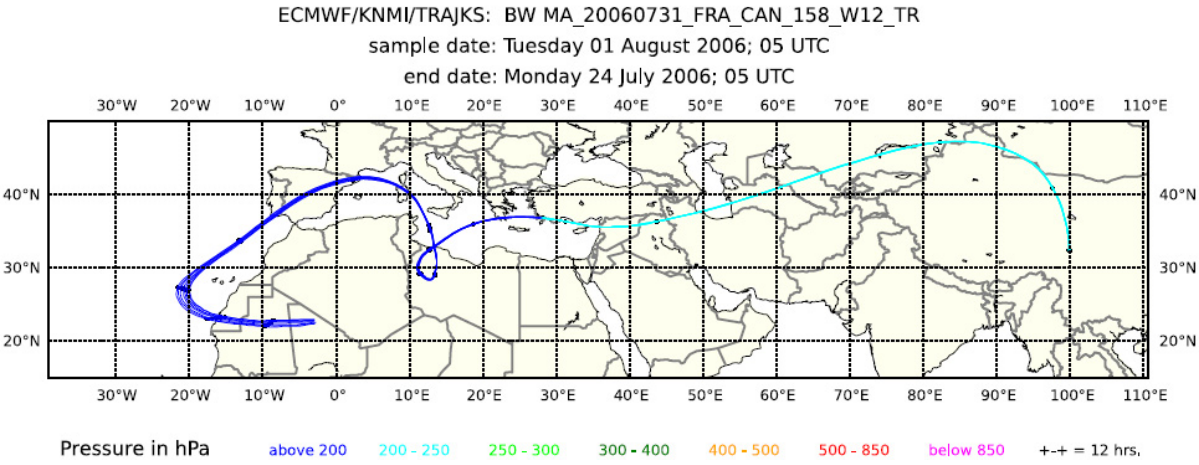

(c)

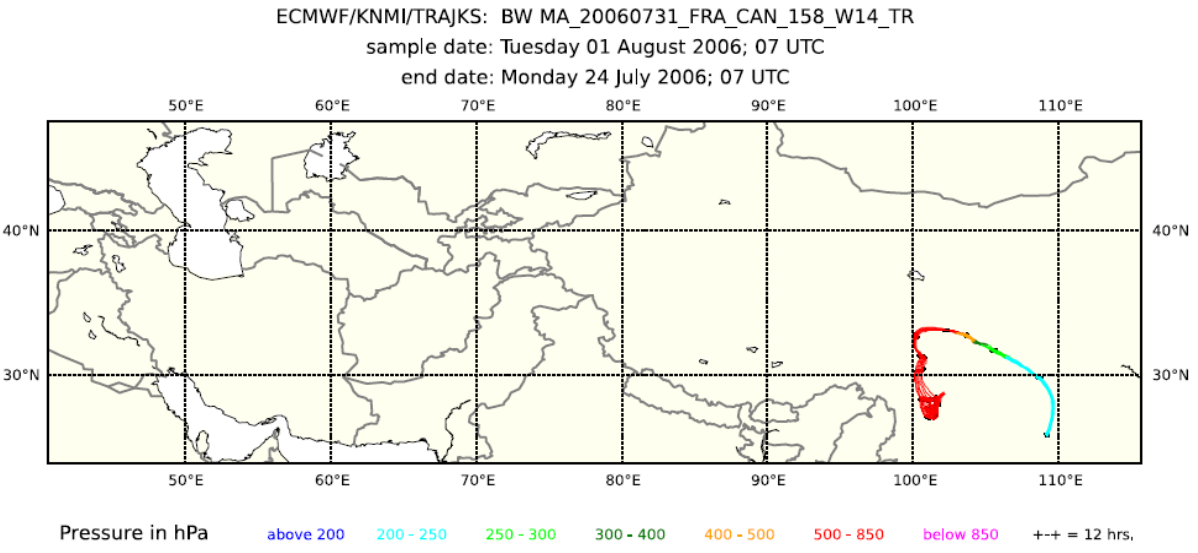

(d)

Figure 5. The overview of the data from Flight 334 from Cape Town to Frankfurt on 21/22 March 2011. The parameters displayed here are similar to those in Figure 2. (**Middle**) The time series plots additionally show the particle surface area concentrations (green); (**second panel from the bottom**) mixing ratios of SF_6 (magenta) and N_2O (green) in whole air samples, as well as continuously measured mixing ratios of CH_4 (dark blue) and CO_2 (light blue); (**bottom**) cloud water content (light blue) and concentrations of particles within the 4–12 nm size range (red) and larger than 12 nm (black).

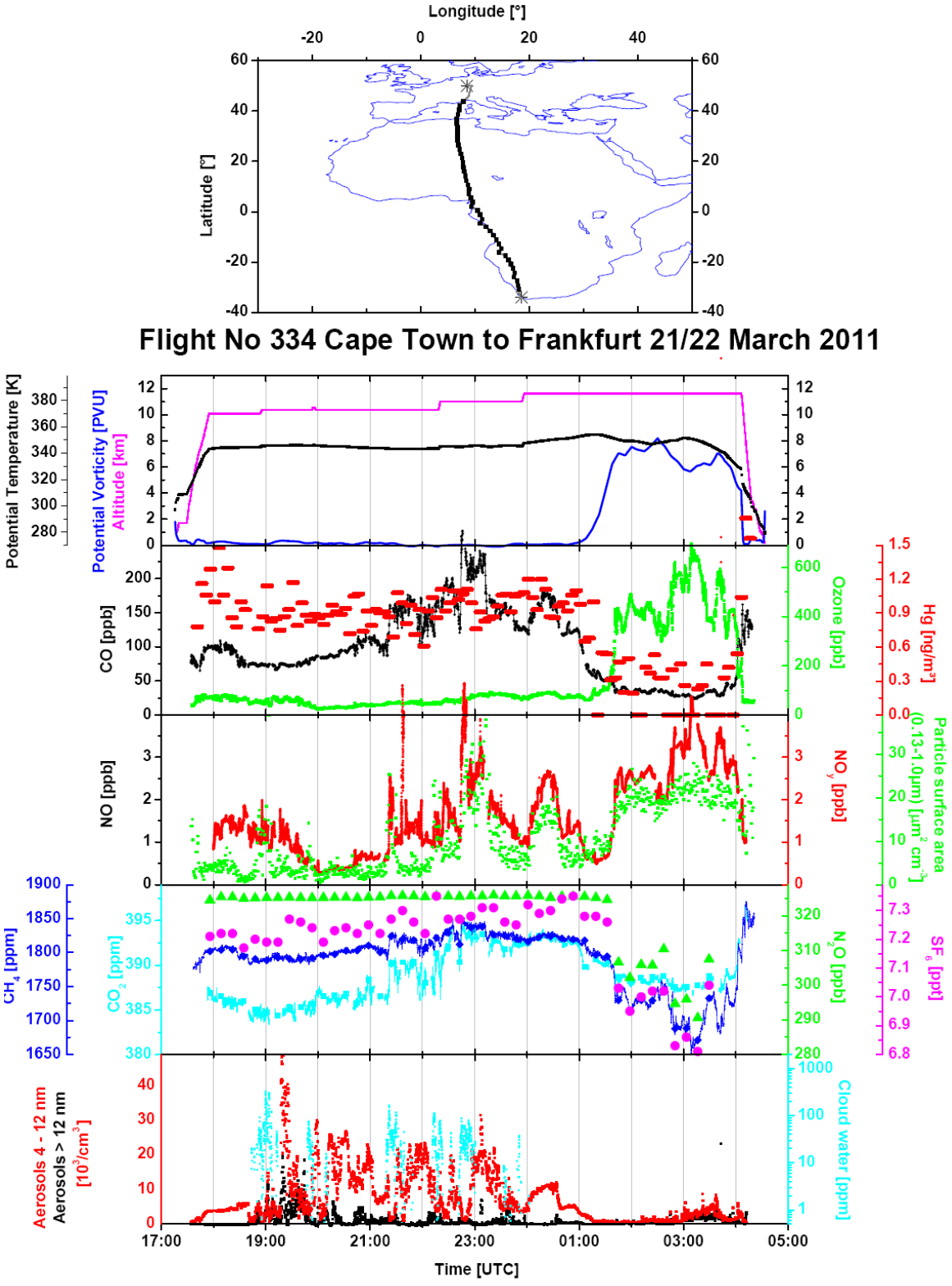

A dense plume observed during Flight 300 from Osaka to Frankfurt on 24 June 2010, covering a distance of about 1000 km over the Korean Peninsula and Yellow Sea, was characterized by CO mixing ratios of ~240 ppb, Hg concentrations of 2.25 ng·m^{-3} and an Hg/CO emission ratio of 4.4 pg·m^{-3}·ppb^{-1}. High mixing ratios of biomass burning tracers, such as CH_3Cl, and of tracers of anthropogenic origin, such as SF_6, together with elevated levels of pollutants, which may originate from both biomass burning and anthropogenic processes, such as ethyne and propane, point to the mixed origin of this plume, both from anthropogenic processes and from biomass burning. Backward trajectories and a map of fire counts for 20–24 June 2010 (not shown, FIRMS (Fire Information for Resource Management System) web fire mapper http://firefly.geog.umd.edu, accessed on 28 October 2010), indicate that the biomass burning component originated most likely from a region with a high burning density in Shandong, Henan, Shanxi and Hebei provinces of China and possibly from some fires in southern Siberia. The anthropogenic component most likely originated from the Chinese provinces mentioned above.

The plumes observed near Osaka during two flights, 331 and 332, on 26/27 February 2011, are characterised by similar CO mixing ratios as in June 2010, but higher Hg concentrations of ~2.7 ng·m^{-3}, resulting in the higher Hg/CO emission ratios of 8.4 and 10.0 pg·m^{-3}·ppb^{-1}, which point to urban/industrial origin. Air samples taken within the plume had elevated mixing ratios of SF_6 (~7.6 ppt), ethyne (~500 ppt), CH_4 (~1870 ppb), CO_2 (~397 ppm) and several other hydrocarbons, documenting the urban/industrial component of the plumes. Biomass burning also contributed to this plume, as evidenced by high CH_3Cl mixing ratios of ~700 ppt. However, the high Hg/CO slope of ~9 pg·m^{-3}·ppb^{-1} and the high SF_6 mixing ratios imply urban/industrial origin to be dominating. Backward trajectories for the plume observed during Flight 331 show a fast transport from the west with surface contact over northern India, southern Pakistan and southern Iran (within ~3 days) and a transport at high altitudes afterwards. Backward trajectories for the plume observed during Flight 332 are similar, but because of their lower altitude contributions from sources in China, cannot be ruled out. However, based on the trajectories from Flight 331 and the low probability of convection in February, we deem northern India and southern Pakistan to be the major source of the observed plumes.

A narrow plume observed during the descent to Seoul during Flight 383 on 29 March 2012, is characterised by very high CO mixing ratios of up to 357 ppb, an Hg concentration of up to 2.49 ng·m^{-3} and an Hg/CO emission ratio of 5.6 pg·m^{-3}·ppb^{-1}. Apart from high NOy and CO_2, there are no other measurements available to characterise this plume. The medium Hg/CO slope indicates a mixture of emissions from biomass burning and industrial/urban emissions. The backward trajectories are changing during the descent and point to northern China or/and southern Siberia as possible source areas.

Several plumes were also encountered over central Asia on the way to Guangzhou and back, especially during Flights 158, 161 (both flights were on 1 August 2006), 166 and 169 (both flights were on 20 October 2006). The events during the outward bound flight on October 20 at 3:53–4:53 UTC and during the return flight on the same day at 17:49–20:29 UTC have very similar Hg/CO emission ratios of 3.5 ± 0.7 and 3.2 ± 1.1 pg·m^{-3}·ppb^{-1}, respectively, and originate, with little doubt, from one and the same plume. This plume is analysed in detail by Baker *et al.* [46]. The low Hg/CO emission ratio and elevated acetonitrile, CH_3Cl and CH_3Br mixing ratios suggest that the plume originates partly from biomass/biofuel burning, whereas elevated mixing ratios of C_2Cl_4 and

toluene, which are used as solvents, indicate anthropogenic contributions. Backward trajectories for the samples taken in this plume pass over Afghanistan, Pakistan and a region of Northern India, where extensive fire activity was recorded during 17–29 October 2006 [46]. Another plume with an Hg/CO emission ratio of 11.2 ± 3.4 pg·m^{-3}·ppb^{-1} and very high acetone mixing ratios was encountered during Flight 161 on 1 August 2006, at 22:07–23:07 UTC. No air samples were taken during this event. Backward trajectories pass at high altitude (<300 hPa) over the Black Sea partly to northern Europe and partly to the European Mediterranean coast. Elevated H_2O mixing ratios and satellite images indicate some convective activity west of the Black Sea. Extensive fire activity was recorded during this time for a broad area along the northern coast of the Black Sea and for the Mediterranean coast.

3.3. Plumes over Africa

Data are available for a total of 13 flights en route between Frankfurt and Cape Town or Johannesburg. As the South African airports were served by Lufthansa Airbus A340-600 aircraft only during the winter flight schedule, the data cover the months from November to March (March 2009–March 2011) encompassing the austral summer. Elevated CO mixing ratios over equatorial Africa were encountered during all flights with peak values varying between ~120 and ~250 ppb, but for only four flights, the Hg *vs.* CO correlation was statistically significant. The reasons for such a low yield are discussed below.

Figure 6. Five-day backward trajectories (every 3 min) for Flight 334 from Cape Town to Frankfurt on 21 and 22 March 2011: (**a**) 21–22 UTC; (**b**) 22–23 UTC; (**c**) 23–24 UTC; and (**d**) 0–1 UTC.

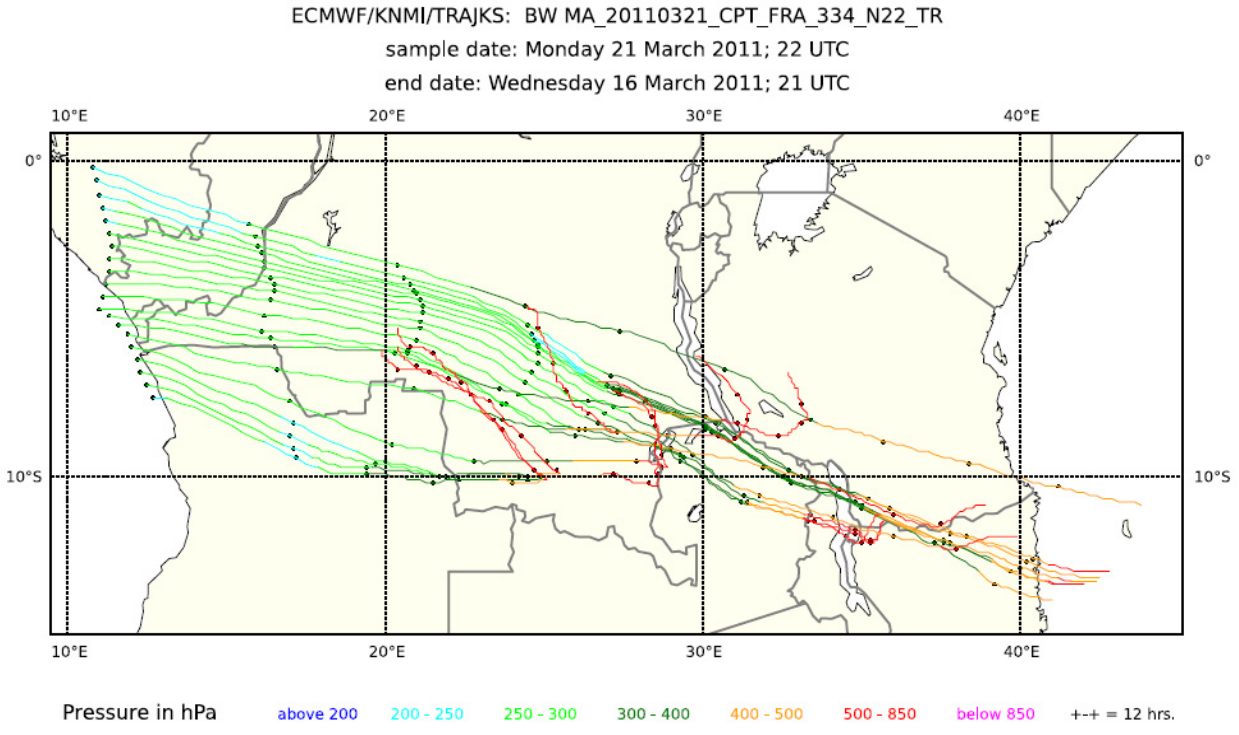

(**a**)

Figure 6. *Cont.*

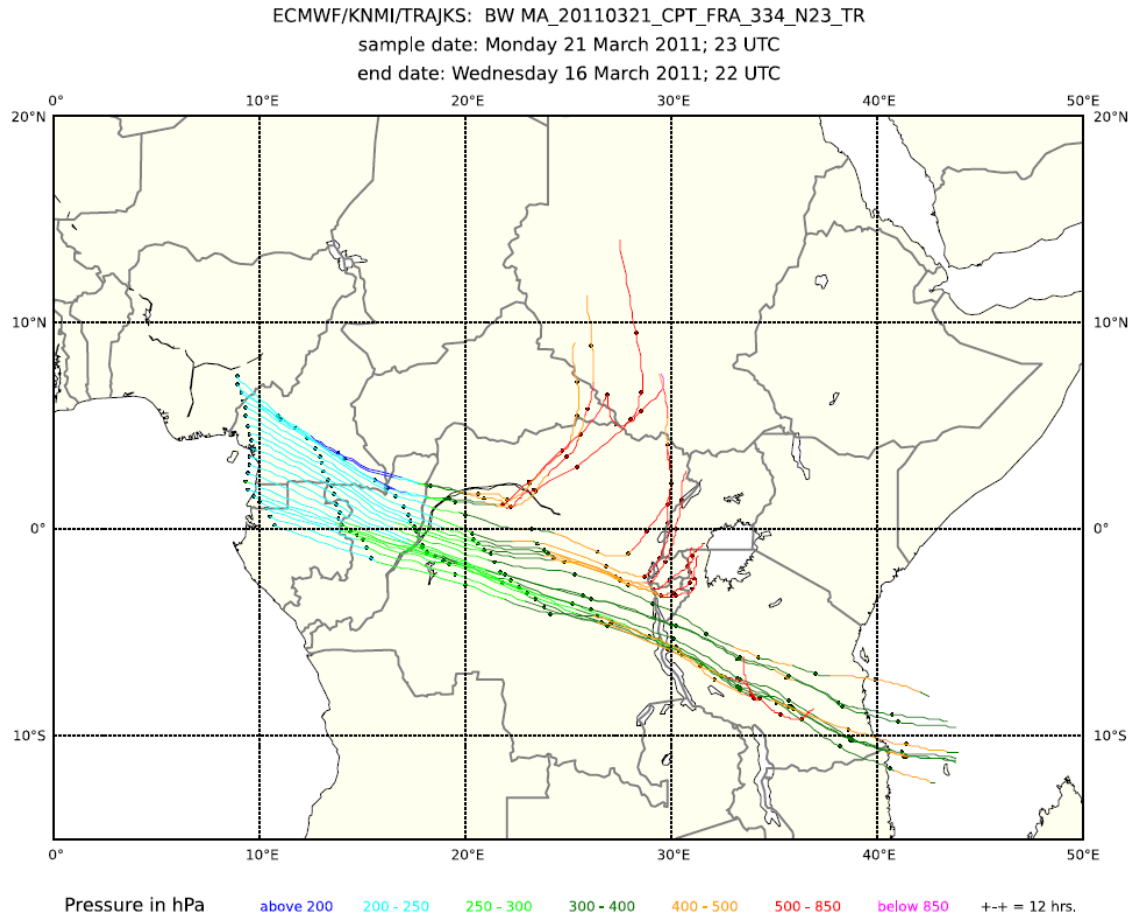

(**b**)

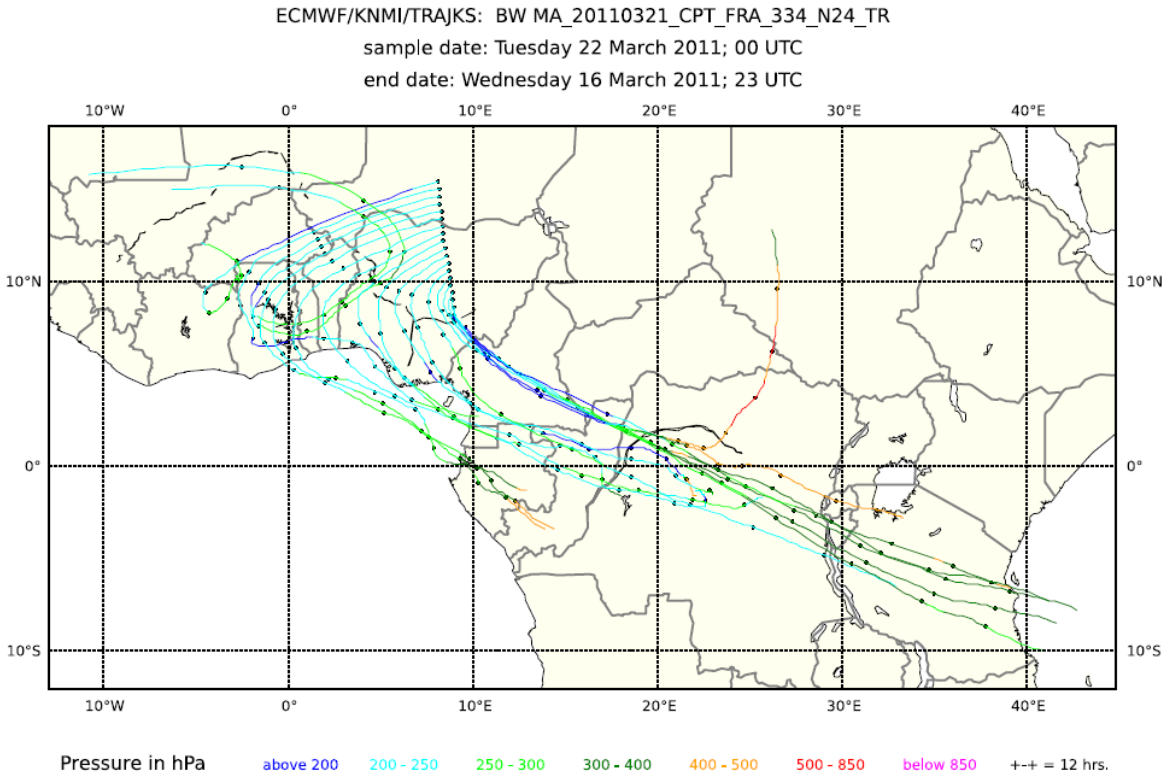

(**c**)

Figure 6. *Cont.*

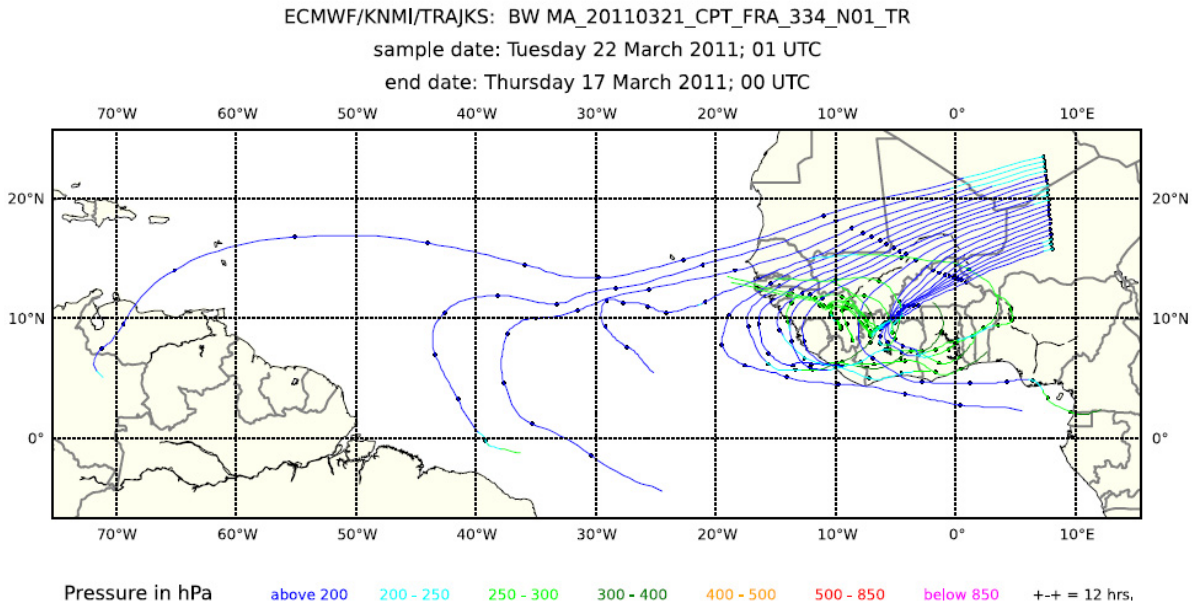

(d)

Figures 5 and S1 show a typical example of the data obtained during Flight 334 from Cape Town to Frankfurt on 20 and 21 March 2011. The second panel from the top of the data time series in Figure 5 shows somewhat elevated CO mixing ratios of ~100 ppb after ascent, decreasing to a southern hemispheric background of ~ 75 ppb after 18:30 UTC. CO then increases in the course of the flight up to a maximum of ~240 ppb between 22:45 and 23:10 UTC to subsequently decrease, with another smaller peak, with a maximum of ~175 ppb around 0:20 UTC, to ~125 ppb, before the aircraft crosses the tropopause into the lower stratosphere at ~1:00 UTC. The NOy mixing ratio and particle surface area concentration (the third panel from the top) display a similar pattern, even in the finer structure, whereas CO_2 and CH_4 show only a broad maximum with a somewhat different shape, peaking shortly before 23:00 UTC. The SF_6 mixing ratio increases gradually from ~7.2 ppt after ascent to ~7.3 ppt before entering the stratosphere. Although small, this increase documents that all plume observations are embedded in a broad gradient between southern and northern hemispheric air masses [47]. Mixing ratios of ethane, propane and ethyne, shown in Figure S1, broadly follow the CO pattern, but high mixing ratios of short-lived n-butane and i-butane around 21:15 UTC and at 23:00 UTC indicate the admixture of freshly polluted air. The CH_3Cl mixing ratio (Figure S1, lowermost panel) of ~ 650 ppt in the tropospheric section of the flight is substantially higher than the background mixing ratio of ~550 ppt, and this implies a large-scale influence of biomass burning. The highest CH_3Cl mixing ratios of almost 700 ppt are found in two samples taken after midnight. They coincide with elevated mixing ratios of CO, ethane, propane, ethyne and NOy (Figure 5, middle panel), but the short-lived butanes have almost disappeared. Such a coincidence is characteristic for aged air from another regional biomass burning plume. Consequently, the CO bulge over equatorial Africa has to be viewed as a composite of several regional plumes. Backward trajectories, shown in Figure 6 for 21–22 UTC (a), 22–23 UTC (b), 23–24 UTC (c) and 0–1 UTC (d), support this view by pointing to different source regions in different sections of the flight. Several of the trajectories exhibit rather fast upward transport from the boundary layer and lower troposphere (purple and red colours). Cloud water content

(Figure 5, bottom panel) in several sections of the flight is a sign of convective activity in these areas. The fire map displayed in Figure 7 and the trajectories show that emissions from biomass burning have, to a varying degree, influenced all observations between ~21:00 UTC on 20 March to ~1:00 UTC on 21 March.

The correlation of Hg *vs.* CO was statistically non-significant for the whole plume starting at 21:16:30 and ending at 01:01:30 UTC, as well as for sections of it, such as between 23:56:30 and 00:56:30 UTC or between 21:21:30 and 23:56:30 UTC. The correlation of Hg *vs.* CO_2 was statistically significant for the whole plume (239.4 ± 94.4 $pg \cdot m^{-3} \cdot ppm^{-1}$ at > 95% level), but statistically non-significant for the sections mentioned above.

Figure 7. The map of fire counts for the period from 12 to 21 March 2011 (http://rapidfire.sci.gsfc.nasa.gov/firemaps/, accessed on 10 October 2013).

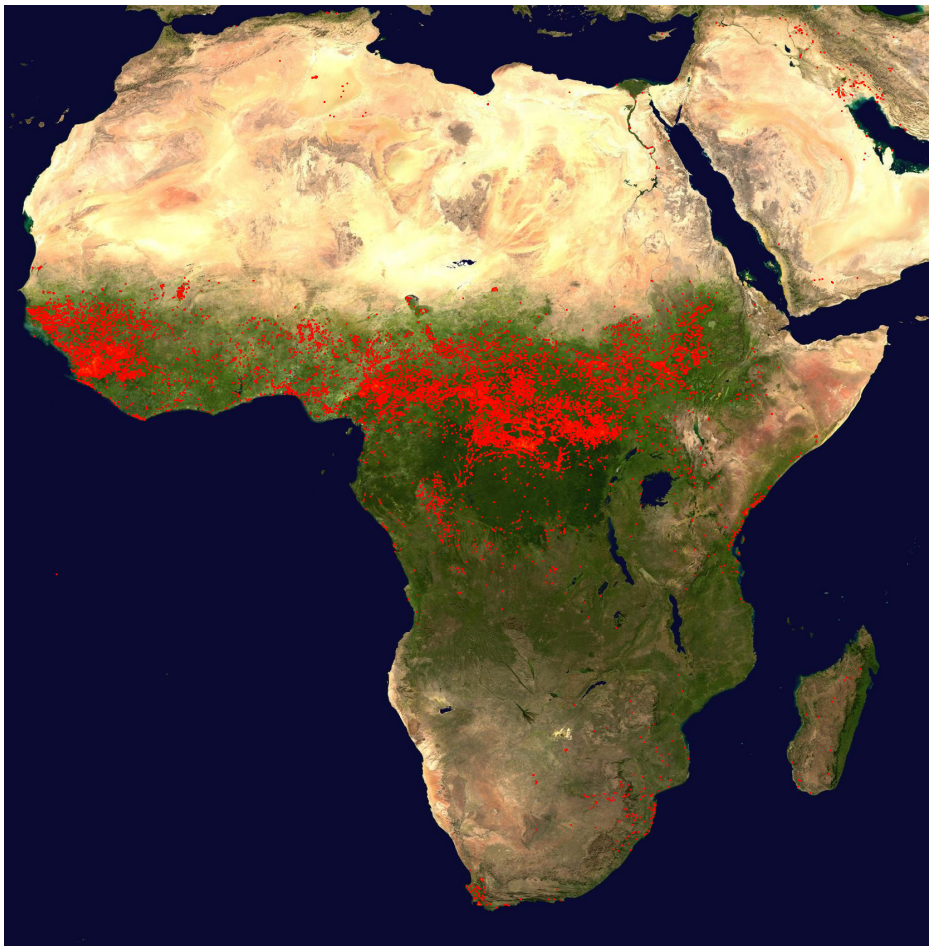

In summary, the scarcity of statistically significant Hg *vs.* CO and Hg *vs.* CO_2 correlations in the plumes observed over equatorial Africa is a result of several factors. The plumes are embedded in broad north-south gradients, which violates the assumption of a constant background. Due to their large extent, they consist of a multitude of overlapping smaller plumes from different regions and sources and are thus not homogeneous. In addition, the CO enhancements (ΔCO) against the background are rather small, varying between ~45 ppb during Flights 290 and 291 to Cape Town on 27 and 28 October 2009, to ~165 ppb during Flights 333 and 334 to Cape Town on 20 and 21 March 2011. Assuming that the plumes originate predominantly from biomass burning with a typical Hg/CO

emission ratio of 1 pg·m^{-3}·ppb^{-1}, the CO enhancements of this magnitude would produce Hg enhancements of only 0.045 to 0.165 ng·m^{-3}. Such enhancements are difficult to detect with a precision of 0.05 ng·m^{-3} of the mercury measurements, even if the background were constant and the plumes homogeneous. For all of these reasons, the Hg/CO emission ratios derived from these flights will be substantially more uncertain than their statistical uncertainty stated in Table S2.

Figure 8. An overview of the data from Flight 348 from Bogotá to Frankfurt on 17 June 2011. The same parameters are displayed as in Figure 5. Additionally, total water content (dark blue) is shown in the bottom panel.

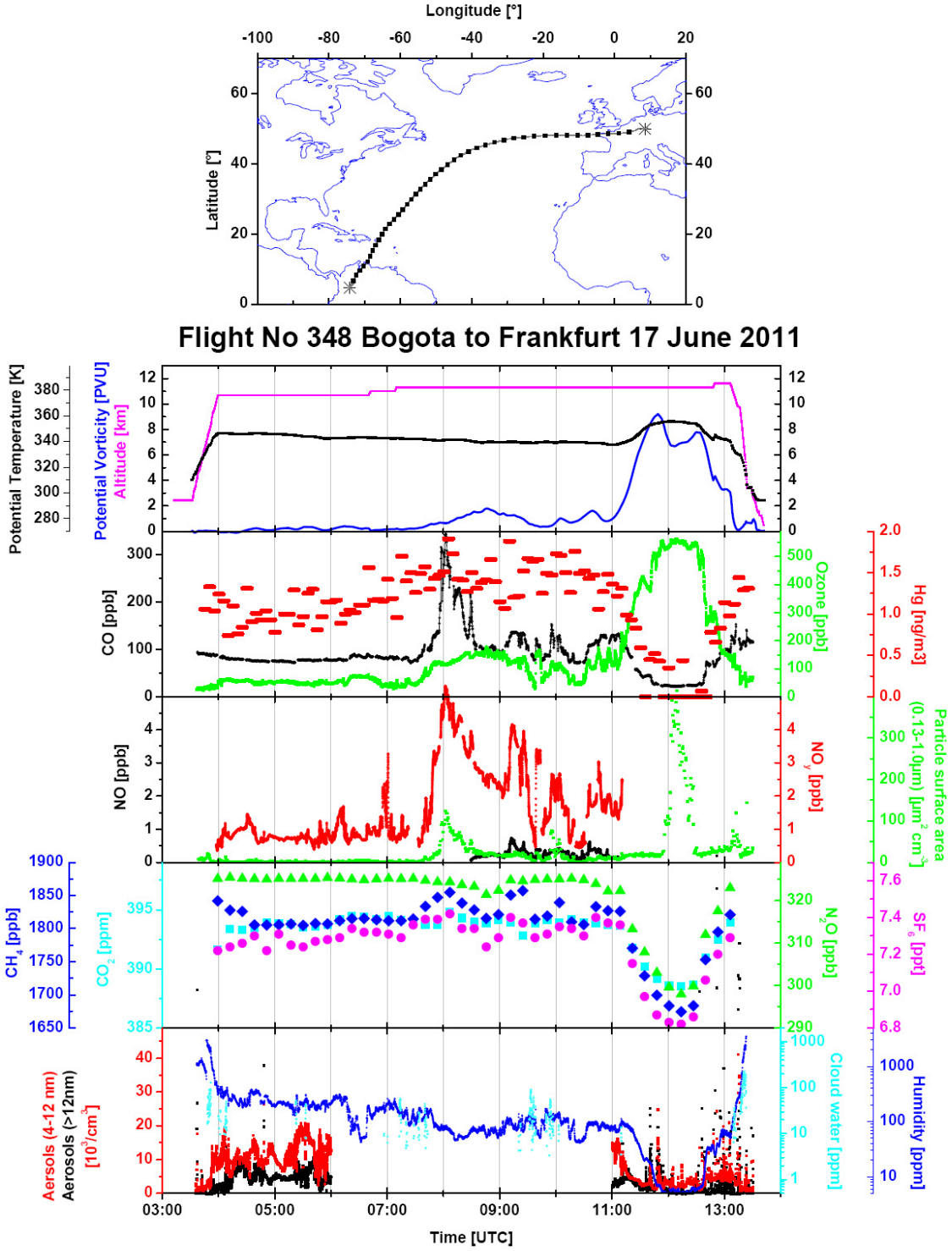

Figure 9. (**a**) eight-day backward trajectories for whole air Sample 6 from the CO peak encountered around 17:20 UTC during Flight 347 from Frankfurt to Bogota on 16 June 2011; and (**b**) for whole air Sample 20 from the CO peak encountered around 8:05 UTC during Flight 348 from Bogota to Frankfurt on 17 June 2011. (**c**) The map of the fire counts for 10–19 June 2011 (http://rapidfire.sci.gsfc.nasa.gov/firemaps/, accessed on 10 October 2013).

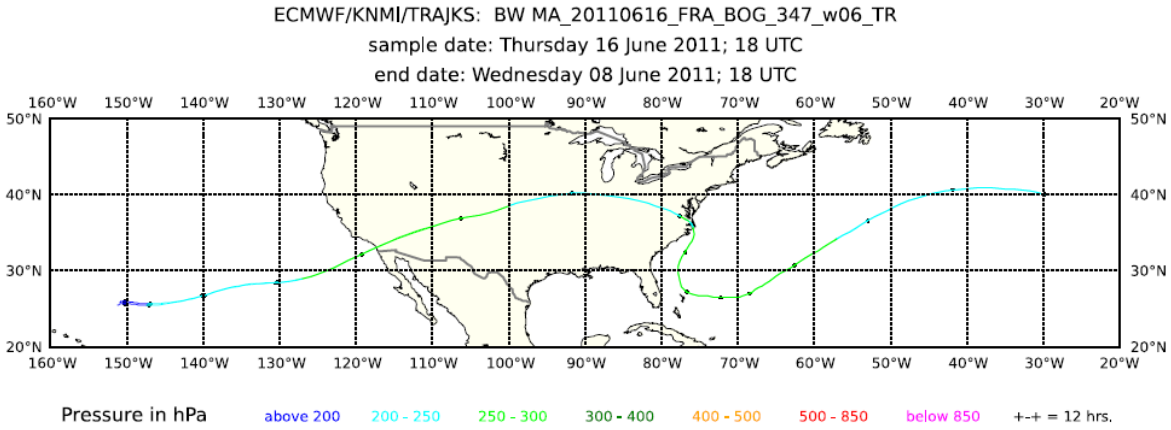

(**a**)

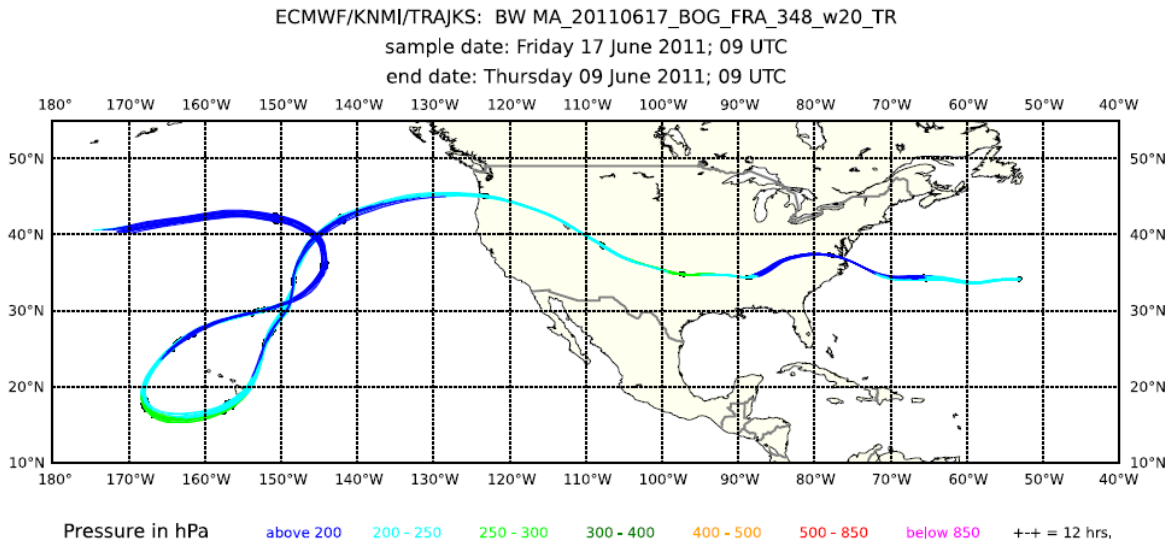

(**b**)

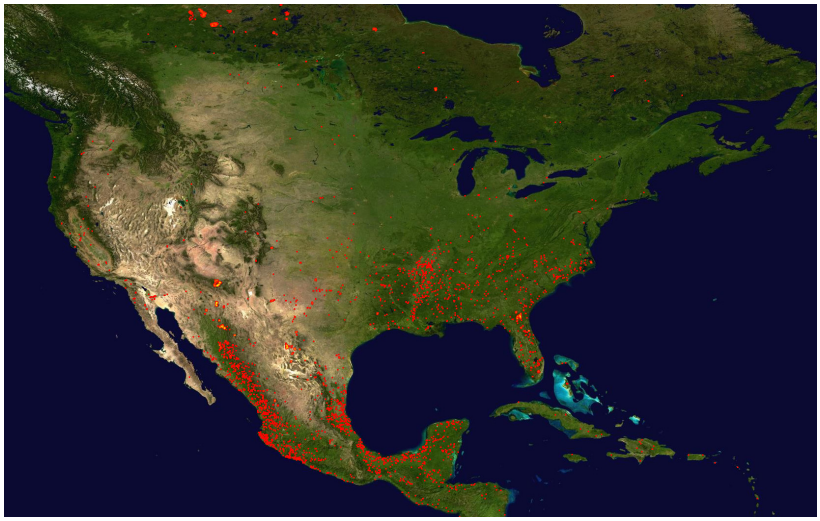

(**c**)

Three of the four statistically significant Hg *vs.* CO correlations for plumes observed over equatorial Africa yield Hg/CO emission ratios of 2.18–3.36 $pg \cdot m^{-3} \cdot ppb^{-1}$, which, again, points to the predominant contribution of emissions from biomass burning.

3.4. Plumes Observed during the Flights to and over South America

The plumes encountered over South America during the flights to São Paulo and Santiago de Chile were analysed in detail by Ebinghaus *et al.* [48]. Here, we would only note that based on their chemical signature, backward trajectories and fire maps, these plumes could be unequivocally attributed to biomass burning in the Amazon Basin and its outskirts.

The encounters at 16:47:30 to 17:47:30 during Flight 347 from Frankfurt to Bogotá on 16 June 2011, and at 7:35:30–8:45:30 during the return Flight 348 on 17 June 2011, both above the middle of the Atlantic Ocean at latitudes ranging from 31° to 43°N, are probably due to the same plume. An overview of the data from Flight 348 (Figure 8) shows a sharp CO peak with ~325 ppb at ~8:00 UTC, accompanied by peaks in NOy, aerosol surface area, CH_4 and a small peak of SF_6, the last one originating from anthropogenic emissions. The CO peak coincides also with the highest CH_3Cl, ethane, propane, n-butane, i-butane and ethyne mixing ratios (Figure S2). The low Hg/CO emission ratios of 1.5 ± 0.6 $pg \cdot m^{-3} \cdot ppb^{-1}$ for this flight and 1.3 ± 0.4 $pg \cdot m^{-3} \cdot ppb^{-1}$ for Flight 347 and the peak CH_3Cl mixing ratio indicate that pollutants from biomass burning are by far the most predominant component of these plumes. Backward trajectories in the upper panel of Figure 9 for Samples 6 and 20, taken within the CO peaks observed during Fights 347 and 348, respectively, show a high level transport from U.S. and north-western Mexico. Satellite cloud images point to convective activity over the south-eastern U.S., the Great Plains and north-western Mexico. The map of fire counts for 10–19 June 2011, in the lower panel of Figure 9, shows that numerous fires in the southeast U.S. might be the major source of the observed plumes, with a possible contribution of fires in Southern California and north-western Mexico.

3.5. Hg/CO_2 Emission Ratios

Hg/CO_2 emission ratios are potentially more useful for constraining the mercury emissions, because CO_2 inventories tend to be more accurate than those of CO [21]. Unfortunately, only a few Hg/CO_2 emission ratios have been reported, so far. Table S3 displays the events with significant Hg *vs.* CO_2 correlations. CO_2 data were available only for 46 plume encounters. Among these, for only 17 encounters, the Hg *vs.* CO_2 correlations were statistically significant (significance level ≥95%). The yield of statistically significant Hg *vs.* CO_2 correlations is thus somewhat smaller than for Hg *vs.* CO, and the significance of these correlations with mostly only 95% tends also to somewhat smaller values. Eleven of the statistically significant correlations were found for plumes with significant Hg *vs.* CO correlations.

The Hg/CO_2 emission ratios vary over a broad range, from 14.4 to 964 $pg \cdot m^{-3} \cdot ppm^{-1}$, and those observed during the flights to East Asian destinations vary between 107 and 964 $pg \cdot m^{-3} \cdot ppm^{-1}$. The Hg/CO_2 emission ratio from the plume observed during Flight 334 to Frankfurt immediately after ascent from Cape Town on 21 March 2011, and during Flight 373 to Chennai after ascent from Frankfurt on 16 January 2012, also fit the range of East Asian plumes. The lowest Hg/CO_2 emission

ratios of 14.4 and 21.9 $pg \cdot m^{-3} \cdot ppm^{-1}$ were both derived from plumes encountered during Flights 329 and 334 over equatorial Africa on 24 February 2011 and 21 March 2011, respectively.

The low Hg/CO_2 emission ratios in the plumes of equatorial Africa are comparable to the median of 34.1 $pg \cdot m^{-3} \cdot ppm^{-1}$ (average: 62.7 ± 80.2 $pg \cdot m^{-3} \cdot ppm^{-1}$) of emission ratios observed in the plumes encountered at Cape Point, which, according to their Hg/CO emission ratios, seem to originate predominantly from biomass burning [21]. The Hg/CO_2 emission ratio from the only plume clearly attributed to biomass burning near Cape Point was somewhat higher with 109 ± 27 $pg \cdot m^{-3} \cdot ppm^{-1}$ [49], but this is comparable to 131 ± 53 $pg \cdot m^{-3} \cdot ppm^{-1}$, observed in the plume from biomass burning in the south-eastern U.S. in June 2011 (Flights 347 and 348). Based on the coal mercury content of 0.15–0.45 $\mu g \cdot Hg \cdot g^{-1}$ and a flue cleaning efficiency for mercury of 50%–90%, Brunke *et al.* [21] predicted an Hg/CO_2 emission ratio to be within the range of 2–30 $pg \cdot m^{-3} \cdot ppm^{-1}$. The Hg content in coal consumed in China varies from 0.027 to 0.369 $\mu g \cdot g^{-1}$ [50] and is not much different from that in South Africa. The flue cleaning efficiency for mercury in China is with up to 57% somewhat lower [50], but this difference cannot explain the Hg/CO_2 emission ratios larger than 100 $pg \cdot m^{-3} \cdot ppm^{-1}$ observed over East Asia, Europe and at Cape Point in South Africa [21]. If confirmed by further measurements, high Hg/CO_2 emission ratios would imply a substantial contribution of emissions from other sources than coal burning.

3.6. Hg/CH_4 Emission Ratios

Mercury also frequently correlated with CH_4 in the plumes observed at Cape Point, and the resulting Hg/CH_4 emission ratios helped to constrain the mercury emissions in South Africa [21]. Continuously measured CH_4 data were available only for 26 plume encounters, and of these, only six provided a statistically significant Hg *vs.* CH_4 correlation at a confidence level of at least 95%. The emission ratios listed in Table S4 vary between 4.8 and 41.4 $pg \cdot m^{-3} \cdot ppb^{-1}$. The only Hg/CH_4 emission ratios available for comparison are derived from observations at Cape Point and are centred in the range of up to 6 $pg \cdot m^{-3} \cdot ppb^{-1}$ [21]. The plume encountered during the flight to Cape Town with an emission ratio of 4.8 $pg \cdot m^{-3} \cdot ppb^{-1}$ falls into this range. All other plumes in Table S4 were of mixed or industrial/urban origin, and they have higher Hg/CH_4 emission ratios.

4. Conclusions

Over 100 plumes with elevated mercury concentrations were encountered during the tropospheric sections of the CARIBIC flights from May 2005, until June 2013. In 98 of them, elevated Hg was accompanied by elevated CO mixing ratios. Several Hg plumes without a simultaneous increase in CO were all encountered over the equatorial Atlantic Ocean during the flights to South America and were attributed to the convection of the marine boundary air at the ITCZ. Hg correlated as statistically significant with CO in more than 50% of the observed plumes and with CO_2 in about 30% of the plumes for which CO_2 data were available. Ample ancillary data on the chemical fingerprint of the air within these plumes and backward trajectories provide additional means to identify the origin and the type of the source.

Extensive mercury plumes over equatorial Africa were observed during all flights between Frankfurt and South Africa. These plumes, which extend over thousands of kilometres, are embedded

in north-south gradients of mercury, CO and CO_2 and consist of a number of overlapping smaller plumes. Due to the changing background, the inhomogeneity of the plumes and the low precision of the Hg measurements, only a few of the plume encounters provided statistically significant Hg *vs.* CO correlations. Most plumes were observed over East Asia, and relative to the number of flights to East Asian destinations, the yield of plumes with statistically significant Hg *vs.* CO correlations was on par with the African flights. Lower yields of plume occurrence were found for flights to South America and to South Asia. Only two plumes were encountered over North America and one over Europe.

The Hg/CO emission ratios derived from these correlations are consistent with the previously published data compiled by Slemr *et al.* [29] and have a smaller values of ~1 $pg \cdot m^{-3} \cdot ppb^{-1}$ for plumes, which we clearly could attribute to biomass burning using backward trajectories, fire count maps and the presence of chemical tracers for biomass burning, such as CH_3Cl and acetonitrile. Larger values of ~6 $pg \cdot m^{-3} \cdot ppb^{-1}$ and more were found for most of the other plumes. Backward trajectories and the presence of man-made tracers, such as C_2Cl_4 and SF_6 in several of these plumes suggest emissions from urban/industrial sources. Both types of chemical tracers were present in several plumes, with Hg/CO emission ratios between 1 and 6 $pg \cdot m^{-3} \cdot ppb^{-1}$, showing their mixed origin.

Many of the plumes were transported over large distances from the area of their origin to the place of their observation. Backward trajectories point to major source areas in equatorial Africa, East Asia, South America and South Asia. The emissions from equatorial Africa and South America are clearly dominated by biomass burning. The East Asian emissions originate from a large area of East Siberia, Korea, China, the Philippines and the Indochinese Peninsula. They are mostly of urban/industrial origin with a varying contribution from biomass and biofuel burning. The South Asian emissions originate mostly from the Indo-Ganges region of northern India. Like the East Asian ones, they are a mixture of emissions from industrial/urban sources and biomass/biofuel burning. Other mercury source areas were also identified: the Middle East, a region along the northern perimeter of the Black Sea, the Mediterranean Sea and the south-western U.S. The Hg/CO emission ratio and the plume fingerprint for the Middle East region suggests industrial/urban emissions to be dominating. The emissions whose origin area was located toward the northern coast of the Black Sea and toward the Mediterranean had both a substantial contribution from biomass burning. Biomass burning was the major component of the emissions from the south-eastern U.S. during one event. We caution that since only a few plumes were attributed to each, the Middle East, Europe and the U.S., no firm conclusions can be drawn for these areas. We note also that the forest fires at northern mid-latitudes occur in summer when convection processes, which carry them to cruising altitudes, are the most active. Consequently, our observations for these areas are biased in favour of biomass burning and neglect emissions in other seasons, such as, e.g., from residential heating in winter.

Only a few Hg/CO_2 and Hg/CH_4 emission ratios have been reported, so far. The range of the Hg/CO_2 emission ratios from the CARIBIC flights is comparable to the range observed at Cape Point [21]. The Hg/CO_2 emission ratios of 107–964 $pg \cdot m^{-3} \cdot ppm^{-1}$ observed in the plumes over East Asia, however, are substantially higher than 2–30 $pg \cdot m^{-3} \cdot ppm^{-1}$, calculated by Brunke *et al.* [21] for coal burning. If confirmed by further measurements, the higher observed than calculated Hg/CO_2 emission ratios would imply other substantial Hg sources in addition to coal burning.

Acknowledgments

We would like to thank Lufthansa and all members of the CARIBIC team for their continued effort to keep running such a complex project. We thank especially Dieter Scharffe, Claus Koeppel and Stefan Weber for the day-to-day maintenance and operation of the CARIBIC container. Funding from the European Community within the GMOS (Global Mercury Observation System) project and from Fraport AG is thankfully acknowledged. We acknowledge the use of FIRMS data and imagery from the Land Atmosphere Near-real time Capability for EOS (LANCE) system operated by the NASA/GSFC/Earth Science Data and Information System (ESDIS) with funding provided by NASA/HQ.

Author Contributions

All authors are members of the CARIBIC team and contributed to the production of the data on which the paper is based. Franz Slemr calculated the emission ratios, and Peter van Velthoven made the meteorological analyses for each flight and calculated the backward trajectories. All authors discussed the results of the manuscript in all stages of its preparation.

Conflicts of Interest

The authors declare no conflict of interest.

References

1. Slemr, F.; Schuster, G.; Seiler, W. Distribution, speciation, and budget of atmospheric mercury. *J. Atmos. Chem*. **1985**, *3*, 407–434.
2. Schroeder, W.H.; Munthe, J. Atmospheric mercury—An overview. *Atmos. Environ*. **1998**, *32*, 809–822.
3. Mergler, D.; Anderson, H.A.; Chan, L.H.M.; Mahaffey, K.R.; Murray, M.; Sakamoto; M.; Stern, A.H. Methyl mercury exposure and health effects in humans: A worldwide concern. *Ambio* **2007**, *36*, 3–11.
4. Scheuhammer, A.M.; Meyer, M.W.; Sandheinrich, M.B.; Murray, M.W. Effects of environmental methylmercury on the health of wild bird, mammals, and fish. *Ambio* **2007**, *36*, 12–18.
5. Nriagu, J.O.; Pacyna, J.M. Quantitative assessment of worldwide contamination of air, water and soils by trace metals. *Nature* **1988**, *333*, 134–139.
6. Nriagu, J.O. A global assessment of natural sources of atmospheric trace metals. *Nature* **1989**, *338*, 47–49.
7. Pirrone, N.; Keeler, G.J.; Nriagu, O. Regional differences in worldwide emissions of mercury to the atmosphere. *Atmos. Environ*. **1996**, *30*, 2981–2987.
8. Pirrone, N.; Allegrini, I.; Keeler, G.J.; Nriagu, J.O.; Rossmann, R.; Robbins, J.A. Historical atmospheric mercury emissions and depositions in North America compared to mercury accumulations in sedimentary records. *Atmos. Environ*. **1998**, *32*, 929–940.

9. Pirrone, N.; Cinnirella, S.; Feng, X.; Finkelman, R.B.; Friedli, H.R.; Leaner, J.; Mason, R.; Mukherjee, A.B.; Stracher, G.; Streets, D.G.; *et al.* Global mercury emissions to the atmosphere from anthropogenic and natural sources. *Atmos. Chem. Phys*. **2010**, *10*, 5951–5964.
10. Pacyna, E.G.; Pacyna, J.M. Global emission of mercury from anthropogenic sources in 1995. *Water Air Soil Pollut*. **2002**, *137*, 149–165.
11. Pacyna, J.M.; Pacyna, E.G.; Steenhuisen, F.; Wilson, S. Mapping 1995 global anthropogenic emissions of mercury. *Atmos. Environ*. **2003**, 37, S109–S117.
12. Pacyna, E.G.; Pacyna, J.M.; Steenhuisen, F.; Wilson, S. Global anthropogenic mercury emission inventory for 2000. *Atmos. Environ*. **2006**, *40*, 4048–4063.
13. Pacyna, E.G.; Pacyna, J.M.; Sundseth, K.; Munthe, J.; Kindbom, K.; Wilson, S.; Steenhuisen, F.; Maxson, P. Global emission of mercury to the atmosphere from anthropogenic sources in 2005 and projections to 2020. *Atmos. Environ*. **2010**, *44*, 2487–2499.
14. Streets, D.G.; Hao, J.; Wu, Y.; Jiang, J.; Chan, M.; Tian, H.; Feng, X. Anthropogenic mercury emissions in China. *Atmos. Environ*. **2005**, *39*, 7789–7806.
15. Streets, D.G.; Zhang, Q.; Wu, Y. Projections of global mercury emissions in 2050. *Environ. Sci. Technol*. **2009**, *43*, 2983–2988.
16. Lin, C.-J.; Pongprueksa, P.; Lindberg, S.E.; Pehkonen, S.O.; Byun, D.; Jang, C. Scientific uncertainties in atmospheric mercury models I: Model science evaluation. *Atmos. Environ*. **2006**, *40*, 2911–2928.
17. Lindberg, S.; Bullock, R.; Ebinghaus, R.; Engstrom, D.; Feng, X.; Fitzgerald, W.; Pirrone, N.; Prestbo, E.; Seigneur, Ch. A synthesis of progress and uncertainties in attributing the sources of mercury in deposition. *Ambio* **2007**, *36*, 19–32.
18. Slemr, F.; Baumbach, G.; Blank, P.; Corsmeier, U.; Fiedler, F.; Friedrich, R.; Habram, M.; Kalthoff, N.; Klemp., D.; Kühlwein, J.; *et al.* Evaluation of modeled spatially and temporarily highly resolved emission inventories of photosmog precursors for the city of Augsburg: The experiment EVA and its major results. *J. Atmos. Chem*. **2002**, *42*, 207–233.
19. Klemp, D.; Mannschreck, K.; Pätz, H.W.; Habram, M.; Matuska, P.; Slemr, F. Determination of anthropogenic emission ratios in the Augsburg area from concentration ratios: results from long-term measurements. *Atmos. Environ*. **2002**, *36*, S61–S80.
20. Jaffe, D.; Prestbo, E.; Swartzendruber, P.; Weiß-Penzias, P.; Kato, S.; Takami, A.; Hatakeyama, S.; Kajii, Y. Export of atmospheric mercury from Asia. *Atmos. Environ*. **2005**, *39*, 3029–3028.
21. Brunke, E.-G.; Ebinghaus, R.; Kock, H.H.; Labuschagne, C.; Slemr, F. Emissions of mercury in southern Africa derived from long-term observations at Cape Point, South Africa. *Atmos. Chem. Phys*. **2012**, *12*, 7465–7474.
22. Slemr, F.; Brunke, E.-G.; Whittlestone, S.; Zahorowski, W.; Ebinghaus, R.; Kock, H.H.; Labuschagne, C. ^{222}Rn-calibrated mercury fluxes from terrestrial surface of southern Africa. *Atmos. Chem. Phys*. **2013**, *13*, 6421–6428.
23. Brenninkmeijer, C.A.M.; Crutzen, P.; Boumard, F.; Dauer, T.; Dix, B.; Ebinghaus, R.; Filippi, D.; Fischer, H.; Franke, H.; Frieß, U.; *et al.* Civil aircraft for the regular investigation of the atmosphere based on an instrumented container: The new CARIBIC system. *Atmos. Chem. Phys*. **2007**, *7*, 1–24.

24. Cooper, O.R.; Moody, J.L.; Parrish, D.D.; Trainer, M.; Ryerson, T.B.; Holloway, J.S.; Hübler, G.; Fehsenfeld, F.C.; Evans, M.J. Trace gas composition of midlatitude cyclones over the western North Atlantic Ocean: A conceptual model. *J. Geophys. Res*. **2002**, doi:10.1029/2001JD000901.
25. Cooper, O.R.; Moody, J.L.; Parrish, D.D.; Trainer, M.; Holloway, J.S.; Hübler, G.; Fehsenfeld, F.C.; Stohl, A. Trace gas composition of of midlatitude cyclones over the western North Atlantic Ocean: A seasonal comparison of O_3 and CO. *J. Geophys. Res*. **2002**, *107*, doi:10.1029/2001JD000902.
26. Dyroff, C.; Zahn, A.; Sanati, S.; Christner, E.; Rauthe-Schöch, A.; Schuck, T.J. Tunable diode laser in-situ CH_4 measurements aboard the CARIBIC passenger aircraft: instrument performance assessment. *Atmos. Meas. Tech. Discuss*. **2013**, *6*, 9225–9261.
27. Schuck, T.J.; Brenninkmeijer, C.A.M; Slemr, F.; Xueref-Remy, I.; Zahn, A. Greenhouse gas analysis of air samples collected onboard CARIBIC passenger aircraft. *Atmos. Meas. Tech*. **2009**, *2*, 449–464.
28. Baker, A.K.; Slemr, F.; Brenninkmeijer, C.A.M. Analysis of non-methane hydrocarbons in air samples collected aboard the CARIBIC passenger aircraft. *Atmos. Meas. Tech*. **2010**, *3*, 311–321.
29. Slemr, F.; Ebinghaus, R.; Brenninkmeijer, C.A.M.; Hermann, M.; Kock, H.H.; Martinsson, B.G.; Schuck, T.; Sprung, D.; van Velthoven, P.; Zahn, A.; *et al.* Gaseous mercury distribution in the upper troposphere and lower stratosphere observed onboard the CARIBIC passenger aircraft. *Atmos. Chem. Phys*. **2009**, *9*, 1957–1969.
30. Talbot, R.; Mao, H.; Scheuer, E.; Dibb, J.; Avery, M.; Browell, E.; Sachse, G.; Vay, S.; Blake, D.; Huey, G.; *et al.* Factors influencing the large-scale distribution of Hg° in the Mexico City area and over the North Pacific. *Atmos. Chem. Phys*. **2008**, *8*, 2103–2114.
31. Neuman, J.A.; Huey, L.G.; Ryerson, T.B.; Fahey, D.W. Study of inlet materials for sampling atmospheric nitric acid. *Environ. Sci. Technol*. **1999**, *33*, 1133–1136.
32. Baron, P.A.; Willeke K. Aerosol *Measurements: Principles Techniques and Applications*; John Wiley and Sons: New York, NY, USA, 2001; pp. 1–1131.
33. Temme, C.; Einax, J.W.; Ebinghaus, R.; Schroeder, W.H. Measurements of atmospheric mercury species at a coastal site in the Antarctic and over the South Atlantic Ocean during polar summer. *Environ. Sci. Technol*. **2003**, *37*, 22–31.
34. Rutter, A.P.; Schauer, J.J. The effect of temperature on the gas-particle partitioning of reactive mercury in atmospheric aerosols. *Atmos. Environ*. **2007**, *41*, 8647–8657.
35. Amos, H.M.; Jacob, D.J.; Holmes, C.D.; Fisher, J.A.; Wang, Q.; Yantosca, R.M.; Corbitt, E.S.; Galarneau, E.; Rutter, A.P.; Gustin, M.S.; *et al.* Gas-particle partitioning of atmospheric Hg(II) and its effects on global mercury deposition. *Atmos. Chem. Phys*. **2012**, *12*, 591–603.
36. Lyman, S.N.; Jaffe, D.A. Formation and fate of oxidized mercury in the upper troposphere and lower stratosphere. *Nat. Geosci*. **2012**, *5*, 114–117.
37. Sprovieri, F.; Pirrone, N.; Ebinghaus, R.; Kock, H.; Dommergue, A: A review of worldwide atmospheric mercury measurements. *Atmos. Chem. Phys*. **2010**, *10*, 8245–8265.
38. Cantrell, C.A. Technical note: Review of methods for linear least-squares fitting of data and application to atmospheric chemistry problems. *Atmos. Chem. Phys*. **2008**, *8*, 5477–5487.

39. Scheele, M.; Siegmund, P.; van Velthoven, P. Sensitivity of trajectories to data resolution and its dependence on the starting point: In or outside a tropopause fold. *Meteorol. Appl*. **1996**, *3*, 267–273.
40. Heue, K.-P.; Brenninkmeijer, C.A.M.; Wagner, T.; Mies, K.; Dix, B.; Frieß, U.; Martinsson, B.G.; Slemr, F.; van Velthoven, P.F.J. Observations of the 2008 Kasatochi volcanic SO_2 plume by CARIBIC aircraft DOAS and the GOME-2 satellite. *Atmos. Chem. Phys*. **2010**, *10*, 4699–4713.
41. Lelieveld, J.; van Aardenne, J.; Fischer, H.; de Reus, M.; Williams, J.; Winkler, P. Increasing ozone over the Atlantic Ocean. *Science* **2004**, *304*, 1483–1487.
42. Kuss, J.; Zülicke, C.; Pohl, C.; Schneider, B. Atlantic mercury emission determined from continuous analysis of the elemental mercury sea-air concentration difference within transects between 50°N and 50°S. *Glob. Biogeochem. Cy.* **2011**, doi:10.1029/2010GB003998.
43. Andreae, M.O.; Merlet, P. Emissions of trace gases and aerosols from biomass burning. *Global Biogeochem. Cy.* **2001**, *15*, 955–966.
44. Mühle, J.; Brenninkmeijer, C.A.M.; Rhee, T.S.; Slemr, F.; Oram, D.E.; Penkett, S.A.; Zahn, A. Biomass burning and fossil fuel signatures in the upper troposphere observed during a CARIBIC flight from Namibia to Germany. *Geophys. Res. Lett*. **2002**, doi:10.1029/2002GL015764.
45. Lai, S.C.; Baker, A.K.; Schuck, T.J.; Slemr, F.; Brenninkmeijer, C.A.M.; van Velthoven, P.; Oram, D.E.; Zahn, A.; Ziereis, H. Characterization and source regions of 51 high-CO events observed during Civil Aircraft for the Regular Investigation of the Atmosphere Based on an Instrument Container (CARIBIC) flights between south China and the Philippines, 2005–2008. *J. Geophys. Res*. **2011**, doi:10.1029/2011JD016375.
46. Baker, A.K.; Traud, S.; Brenninkmeijer, C.A.M.; Hoor, P.; Neumaier, M.; Oram, D.E.; Rauthe-Schöch, A.; Sprung, D.; Schloegl, S.; Slemr, F.; *et al.* Pollution pattern in the upper troposphere over Europe/West Asia and Asia observed by CARIBIC. *Atmos. Environ*. **2014**, in press.
47. Maiss, M.; Steele, L.P.; Francey, R.J.; Fraser P.J.; Langenfelds, R.L.; Trivett, N.B.A.; Levin, I. Sulfur hexafluoride—A powerful new atmospheric tracer. *Atmos. Environ*. **1996**, *30*, 1621–1629.
48. Ebinghaus, R.; Slemr, F.; Brenninkmeijer, C.A.M.; van Velthoven, P.; Zahn, A.; Hermann, M.; O'Sullivan, D.A.; Oram, D.E. Emissions of gaseous mercury from biomass burning in South America in 2005 observed during CARIBIC flights. *Geophys. Res. Lett*. **2007**, doi:10.1029/2006GL028866.
49. Brunke, E.-G.; Labuschagne, C.; Slemr, F. Gaseous mercury emissions from a fire in the Cape Peninsula, South Africa, during January 2000. *Geophys. Res. Lett*. **2001**, *28*, 1483–1486.
50. Tian, H.Z.; Wang, Y.; Xue, Z.G.; Cheng, K.; Qu, Y.P.; Chai, F.H.; Hao, J.M. Trend and characteristics of atmospheric emissions of Hg, As, and Se from coal combustion in China, 1980–2007. *Atmos. Chem. Phys*. **2010**, *10*, 11905–11919.